Development of a Meso-scale Multi-axis Magnetic Tactile Sensor for Robotic Surgery

Author

Muhammad Rehan

00000317665

Supervisor

Dr. Muhammad Mubasher Saleem

DEPARTMENT OF MECHATRONICS ENGINEERING

COLLEGE OF ELECTRICAL & MECHANICAL ENGINEERING

NATIONAL UNIVERSITY OF SCIENCES AND TECHNOLOGY

ISLAMABAD

August 2022

Development of a Meso-scale Multi-axis Magnetic Tactile Sensor for Robotic Surgery

Author

Muhammad Rehan

00000317665

A thesis submitted in partial fulfillment of the requirements for the degree of

MS Mechatronics Engineering

Thesis Supervisor:

DR. MUHAMMAD MUBASHER SALEEM

Thesis Supervisor's Signature:

_____

DEPARTMENT OF MECHATRONICS ENGINEERING

COLLEGE OF ELECTRICAL & MECHANICAL ENGINEERING

NATIONAL UNIVERSITY OF SCIENCES AND TECHNOLOGY,

ISLAMABAD

August 2022

Declaration

I certify that this research work titled "*Development of a Meso-scale Multi-axis Magnetic Tactile Sensor for Robotic Surgery"* is my own work. The work has not been presented elsewhere for assessment. The material that has been used from other sources has been properly acknowledged/referred to.

Signature of Student

Muhammad Rehan

00000317665

Language Correctness Certificate

This thesis has been read by an English expert and is free of typing, syntax, semantic, grammatical and spelling mistakes. The thesis is also according to the format given by the university.

Signature of Student

Muhammad Rehan

00000317665

Signature of Supervisor

Copyright Statement

Acknowledgments

I am utmost grateful to Almighty Allah, the most powerful and merciful. He has always guided me towards the right objectives in life. After the Lord, I am thankful to my loving parents and siblings for their consistent motivation and support in accomplishing goals throughout my life while remaining optimistic.

I heartily appreciate the efforts of my master's supervisor Dr. Muhammad Mubasher Saleem, Associate Professor and Associate Head of the Department of Mechatronics Engineering, College of Electrial and Mechanical Engineering, NUST. I am thankful for his counselling and mentoring in developing my interest in a research field. His incredible devotion in the research and development phase of this project has made it possible to complete the project timely. I have benefited from his guidance during the work, which kept me on track while learning the research process, increasing my knowledge, and polishing my skills.

I am thankful to my GEC members, Dr. Mohsin Islam Tiwana and Dr. Hamid Jabbar as well, for their time and guidance in my research project.

Finally, I thank my friends, colleagues and staff in the project lab who always responded and provided me with the necessary support during the project.

I would like to dedicate this work to my exceptional parents, grandparents, late uncle and loving siblings whose tremendous support and cooperation led me to this wonderful accomplishment.

List of Journal/Conference Paper Published

- Rehan, Muhammad, Muhammad Mubasher Saleem, Mohsin Islam Tiwana, Rana Iqtidar Shakoor, and Rebecca Cheung. 2022. "A Soft Multi-Axis High Force Range Magnetic Tactile Sensor for Force Feedback in Robotic Surgical Systems" *Sensors* 22, no. 9: 3500. https://doi.org/10.3390/s22093500

Abstract

Robotic surgical procedures have gained a lot more importance in the previous years. The major limitation of surgical robotic systems is that they lack sense of tactile force feedback during object grasping and tissue manipulation. To increase the awareness of surgical robotic systems a magnetic transduction mechanism based tactile force sensor is proposed. Tactile force sensors developed to date lacked the capability to detect multi-axial forces, flexibility, high dynamic and static force range and frequency response. This thesis aims to address the afore mentioned limitations using design optimization through FEM simulations, decoupling of force using mathematical model and by testing the sensor according to real time applications. The magnetic tactile sensor consists of four SMD Hall sensors with four magnets embedded in the soft elastomer. The movement of magnets due to the applied force causes the change in magnetic flux and thus causing a voltage change in the Hall sensors. FEM simulations are carried out for robust location estimation of the embedded magnets in the elastomer. The sensor is fabricated using two types of elastomers based on their stiffness values. The sensor having elastomer as Ecoflex 00-30 works well for a normal force of 20 N in this direction, 3.5 N in shear direction and 1.5 N in angular direction with sensitivities of 16 mV/N, 30 mV/N and 81 mV/N for normal and shear angular force directions respectively. Similarly, the sensor having elastomer as RTV-528 silicone rubber is works well for a force range of 50 N in normal direction, 5.5 N in shear direction and 4 N in angular direction with sensitivities of 2.52 mV/N, 3.4 mV/N and 25 mV/N for normal, shear and angular directions respectively. To assess behaviour of sensor for the dynamic input force the proposed sensor is also tested for the frequency of 4 Hz. The proposed magnetic tactile sensor shows perfectly linear behaviour with a low hysteresis error value of 8.3% and for the repeatability test of the sensor an error of 6.4% is achieved.

Key Words: *Tactile sensor, multi-axis, force sensor, soft sensor, magnetic field, finite element method, robotic surgery, force range, elastomer, Hall sensors.*

Table of Contents

Declaration ..... **i**

Language Correctness Certificate ..... **ii**

Copyright Statement ..... **iii**

Acknowledgments ..... **iv**

List of Journal/Conference Paper Published ..... **vi**

Abstract ..... **vii**

Table of Contents ..... **viii**

List of Figures ..... **xi**

List of Tables ..... **xiv**

Acronyms ..... **xv**

Chapter 1: Introduction **16**

1.1 Aim and Objectives 17

1.2 Minimally Invasive Robotic Surgery (MIRS) 17

1.3 Tactile Sensors and their Types 20

1.4 Characteristics of a Tactile Sensor considering Robotic Surgical System 20

1.5 Application of Tactile Force Sensors in Robotic Surgical Systems 21

Chapter 2: Literature Review **23**

2.1 Tactile Force Sensors based on Different Transduction Mechanisms 23

2.1.1 Capacitive Tactile Force Sensors 23

2.1.2 Piezoelectric Tactile Force Sensors 24

2.1.3 Piezoresistive Tactile Force Sensor 25

2.1.4 Inductive Tactile Force Sensors 26

2.1.5 Optical Tactile Force Sensor 27

2.1.6 Magnetic Tactile Force Sensor 28
2.2 Comparison of Transduction Mechanisms for Tactile Force Sensing 30
2.3 Limitations of the Magnetic Tactile Force Sensors in the Literature 32
2.4 Characteristics of the Proposed Sensor 32
2.5 Force Requirements for Surgical procedures 32
Chapter 3: Sensor Development 34
3.1 Design and Working Principle of the Sensor 34
3.1.1 Design 34
3.1.2 Working Principle 35
3.2 Sensor Schematics and PCB Design 36
3.3 Sensor Fabrication 37
3.3.1 Cost Analysis 38
3.4 Sensor Modelling 39
3.4.1 FEM Modelling 39
3.4.2 Mathematical Modelling 42
Chapter 4: Experimentation and Results 44
4.1 Experimental Setup 44
4.2 LabView Setup and GUI 45
4.3 Testing and Results 47
4.3.1 Sensor with Ecoflex 00-30 Elastomer 48
4.3.2 Sensor with RTV-528 Elastomer 52
4.3.3 Dynamic Response 54
4.3.4 Repeatability Test 55
4.3.5 Hysteresis Test 56
4.4 Sensor Calibration based on Experimental Voltage Output 56
4.5 Summary of Performance Characteristics 58
4.6 Discussion 59

4.7 Applications and Future Work 62

4.8 Limitations of the Proposed Sensor..... 62

Chapter 5: Conclusion 64

References 65

Completion Certificate..... 72

Thesis Acceptance Certificate 73

List of Figures

Figure 1.1 Minimally Invasive Robotic Surgery (MIRS) using da Vinci^{TM} system [14] 19
Figure 1.2 Damage caused to a colon tissue due to excessive pressure exertion during grasping with a surgical gripper [15] 20
Figure 1.3 A wearable tactile sensor for object grasping feedback [17] 21
Figure 1.4 A remote palpation probe with integrated tactile force sensor at the jaws of gripper [18] 21
Figure 1.5 Research map of the thesis 22
Figure 2.1 (a) Schematics of a capacitive tactile force sensor [21] **(b)** Working principle of capacitive tactile force sensor **(c)** Design of a capacitive tactile force sensor with single top electrode [22] 24
Figure 2.2 (a) PVDF films mounted on a gripper acting as piezoelectric tactile force sensor [23] (b) MEMS based piezoelectric tactile force sensor mounted on endoscopic probe [24] **(c)** Piezo electric tactile force sensor mounted on catheter tip [24] 25
Figure 2.3 (a) Micro strain gauges mounted at grippers with a feedback system for estimating input force [27] **(b)** Flexi force sensors mounted on forceps of daVinci surgical robot [28]. 26
Figure 2.4 (a) A tri-axis inductive tactile force sensor [29] **(b)** Working principle of eddy current 27
Figure 2.5 (a) Optical tactile force sensor based on bionic eye compound [31] **(b)** A fiber optic-based MEMS force tactile sensor [32] 27
Figure 2.6 Tactile force sensors working on magnetic transduction principle presented in the literature based on single-axis and tri-axis Hall sensors [35][37][39][40][43] 30
Figure 3.1 Schematics of the proposed sensor **(a)** Top-view **(b)** Cross-section view 35
Figure 3.2 Electrical schematic design of the sensor PCB 36
Figure 3.3 PCB design of the proposed sensor 37
Figure 3.4 Exploded design of the proposed sensor 38
Figure 3.5 (a) Ecoflex 00-30 **(b)** PCB with Hall sensors mounted and 3D printed moulds **(c)** Cylindrical magnets and shaped elastomer on assembled PCB **(d)** Silicone rubber (RTV-528), 3D printed moulds and fibre sheet **(e)** Fabricated sensor. 38
Figure 3.6 Fabricated sensor with a reference object for size estimation 39

Figure 3.7 Cylindrical magnets embedded in the elastomer emitting magnetic field lines 40
Figure 3.8 (a) Mean magnetic flux across all Hall sensors towards an input normal force **(b)** Magnetic flux across RX Hall sensor and LX Hall sensor due to a +x direction input shear force. 41
Figure 3.9 Displacement of the proposed sensor simulated using FEM environment 42
Figure 4.1 USB 6009 DAC device from National Instruments 44
Figure 4.2 Experimental testing and data acquisition setup 45
Figure 4.3 LabView block diagram for real time data acquisition of sensor 46
Figure 4.4 LabView block diagram for data logging of the sensor values 46
Figure 4.5 LabView GUI for acquisition of the sensor 47
Figure 4.6 Force illustration for octagonal dome 47
Figure 4.7 Force application on the sensor face using the force gauge probe 48
Figure 4.8 Displacement of sensor in normal direction for an input applied force of 20N 48
Figure 4.9 Voltage output of the proposed sensor with Ecoflex 00-30 elastomer for a normal force 49
Figure 4.10 Voltage output of the proposed sensor with Ecoflex 00-30 elastomer for a shear force (+x) 50
Figure 4.11 Voltage output of the proposed sensor with Ecoflex 00-30 elastomer for an angular force (45°) 51
Figure 4.12 Voltage output of the proposed sensor with Ecoflex 00-30 elastomer for input angular forces 52
Figure 4.13 Voltage output of the proposed sensor having RTV-528 as elastomer for an input normal force 53
Figure 4.14 Voltage output of the proposed sensor having RTV-528 as elastomer for +x-direction input shear force 53
Figure 4.15 Voltage output of the proposed sensor having RTV-528 as elastomer for an input force at 45° 54
Figure 4.16 Voltage output of the proposed sensor for a dynamic normal force of 10 N 55
Figure 4.17 Repeatability test of the proposed sensor for a normal force up to 20 N 55

Figure 4.18 Hysteresis of the proposed sensor for a force in normal direction 56
Figure 4.19 Applied versus measured force in the normal direction 57
Figure 4.20 Applied versus measured force in the shear direction 58

List of Tables

Table 2.1 Different transduction mechanisms and their comparison [12,47,48] 31
Table 2.2 Force requirements in different surgical practices [50]..... 33
Table 3.1 Magnetic field density towards applied force 36
Table 3.2 Cost breakdown for the proposed sensor 39
Table 4.1 Performance parameters of the proposed sensors 59
Table 4.2 Comparison of the proposed sensor with the literature..... 61

Acronyms

PCB	Printed Circuit Board
FEM	Finite Element Method
MIS	Minimally Invasive Surgery
MIRS	Minimally Invasive Robotic Surgery
PDMS	Polydimethylsiloxane
PVDF	Polyvinylidene Fluoride or Polyvinylidene Difluoride
MEMS	Microelectromechanical Systems
PLA	Poly Lactic Acid
2D	Two Dimensional
3D	Three Dimensional
CAD	Computer Aided Design
RTV	Room Temperature Vulcanizing
CTS	Capacitive Tactile Sensor
SMT	Surface Mounting Technology
SMD	Surface Mounting Device
CNC	Computerized Numeric Control
DAC	Data Acquisition and Control
ADC	Analog to Digital Converter
GUI	Graphical User Interface

Chapter 1: Introduction

In many natural systems, the sense of touch, also known as tactile sensing, is critical for manipulative and exploratory tasks. In humans, even a temporary loss of touch in the fingers due to cold makes a simple task like buttoning a shirt difficult. Tactile sensing, in general, uses physical contact to provide information about shape, temperature, texture, shear and normal forces, pressure, and vibrations. Despite the importance of tactile sensing in nature, it is not present in current robotic systems. Tactile feedback would allow dexterous manipulation of objects as well as detection of textures and other physical stimuli in humanoid robots and prosthetics [1]. Tactile feedback via medical instruments could also be used in minimally invasive surgery (MIS) to detect anatomical changes caused by diseases, such as tumors, kidney stones, and arterial stenosis [2].

Robot-assisted surgeries have gained a lot more importance in previous years. There are many surgical robots that are commercially available and that can perform the procedures such as laparoscopic surgeries, ocular surgeries and cancerous tissue removal. Whereas the major limitation of these robotic surgical systems is the loss of tactile force feedback during the surgical procedure, which can cause damage to tissue or organ during the procedure and there is a chance of trauma and blood loss. To improve the efficiency of the surgical robotic systems there is a dire need for a force feedback system for robot-assisted surgeries and minimally invasive robotic surgeries (MIRS). This chapter focuses on the benefits and limitations of minimally invasive robotic surgeries, types of tactile feedback and different application of tactile force sensors with surgical tools and systems. The review in Chapter 2 reveals that current technology fails to address the following limitations and constraints while attempting to achieve tactile perception or force feedback: -

- Tactile force sensors with detection capabilities of shear and angular forces and decoupling them.
- Tactile force sensors with appropriate sensitivities, resolution, dynamic range, and frequency response.
- Tactile force sensors that are physically soft, modular, robust and low cost.

- Tactile force sensors and electronics that consider wiring and signal readout to make robotic surgical systems easier to integrate.

1.1 Aim and Objectives

A detailed literature review which is summarised in Chapter 2, shows that there have been many attempts in recent times to restore tactile force feedback in MIS and MIRS, but many have not yielded clinically acceptable results due to their own limitations. A tactile force feedback system is made up of two different parts: a sensor that collects surface data and a stimulant actuator or display that transmits and displays that data towards the surgeon console. Because these two setups are completely different components that aren't built with the same technology, their development requires a different set of skills, abilities, and expertise. These various requirements are rarely found in a single research group, making the task of developing an adequate tactile feedback system extremely difficult. The aim of this thesis is to develop a magnetic field transduction mechanism-based tactile force sensor for surgical robotic systems. The objectives of this thesis include design validation, fabrication and characterization of the sensor keeping in view the application of robotic surgery.

1.2 Minimally Invasive Robotic Surgery (MIRS)

Robots have gained a lot of importance in the medical field and surgical procedures. MIS is a procedure in which a surgeon uses small skin incisions to access the internal anatomy of the human body to perform any operation and when a robot assists in this procedure it is referred to as minimally invasive robotic surgery (MIRS). By using the MIRS technique, the anesthesia time for operation, loss of blood during the procedures and trauma is reduced and the overall recovery time of the patient is also minimized. The commercially available MIRS systems include the ZEUS^{TM} and the da Vinci^{TM} robotic surgical systems [3], [4]. As shown in Figure 1.1 the robotic surgical systems have master-slave consoles, the master console is for the surgeon to operate the tools and the slave console is at the patient side for procedures using tools. MIRS has many benefits for the surgeon also because it requires less effort, and the output of the surgery or procedure is also up to the marks. The limitation of these robotic surgical systems is that the surgeon is unable to get an idea of how much grasping force is being exerted during tissue manipulation or any other procedure because the skin incision is

very small, and this may cause extensive force application and may damage organs as well. In conventional surgery methods, the sense of touch plays an important role and to achieve this in MIS and MIRS the utilization of flexible tactile sensors for medical surgery and robotic manipulations has made it possible [5], [6]. da Vinci^{TM} surgical robot is the first and most successful commercially available surgical robot also doesn't provide force feedback or tactile feedback and it has also been reported that by using force feedback during the grasping applications using the da Vinci^{TM} robot the grasping force can be reduced [7]. The estimation of tool tissue interaction forces during the MIRS is still a challenge and requires a new method to acquire force feedback [8].

The worst thing that can happen during surgery is causing harm during the procedure. The opposing argument is that avoiding harm is the most important thing. As arteries are hidden in some tissues and cutting them can be critical therefore there is a high risk of causing harm to arteries during the procedures of MIS and MIRS. This risk is minimal in open surgery because the surgeon can palpate and sense the hidden arteries. A pressurized vessel can always be detected by feeling a light pulse within tissues with the fingertip. Thus, a surgeon will palpate any unknown tissue before performing a blunt dissection to avoid uncontrolled bleeding risk and trauma [1], [2]. This is impossible in MIS because there is no close exposure with the tissue under the procedure, and even more so in MIRS because the patient and surgeon are separated mechanically. There is always the possibility of damaging an artery. Unintended bleeding in MIS and MIRS is also an issue and stopping it takes longer because it is more time-consuming than open surgery. Blood can also contaminate the endoscope, potentially causing complete blindness and forcing the surgeon to switch to open surgery during the procedure, causing time delays and possibly putting the patient's life in danger. Figure 1.2 shows the damage cause to a colon tissue during the surgical procedure. The problem's relevance is demonstrated by the following three examples:

- A known, serious complication of laparoscopic hernioplasty (inguinal hernia repair) using MIS is laceration of the epigastric arteries, which can result in severe bleeding [9]–[11]. Because the iliac and femoral vessels are specifically affected [11], the patient may lose a leg. This is especially important because inguinal hernia surgery is one of the most common procedures, at least in Germany and the United States [12].

- Another frequently performed procedure is cholecystectomy (gall bladder removal). More than 80% of procedures in modern health care are minimally invasive [13]. Due to anatomical variations, bleeding of the cystic and/or proper hepatic arteries, as well as lesions of vascular structures within the hepato-duodenal ligament, are common complications. In this case, complications may increase, and an MIS may be required to be converted to open surgery.
- In minimally invasive surgery, there is currently no method for locating invisible arteries. Their forces are too low for force feedback detection, and the covering tissue prevents optical discovery. This is not only inconvenient for the surgeon, but it also poses a serious risk to the patient due to the possibility of damaging a hidden artery. Even in standard procedures, a possible check for hidden arteries before any dissection can improve patient safety and surgery quality.[14]

Figure 1.1 Minimally Invasive Robotic Surgery (MIRS) using da Vinci^{TM} system [14]

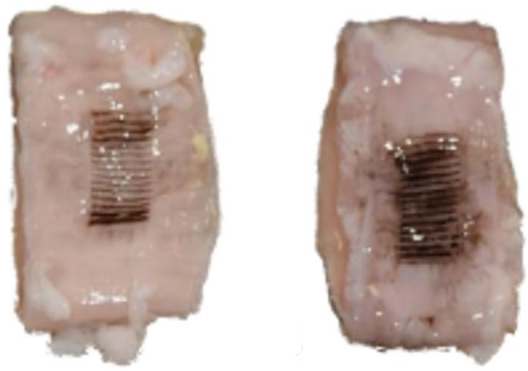

Figure 1.2 Damage caused to a colon tissue due to excessive pressure exertion during grasping with a surgical gripper [15]

1.3 Tactile Sensors and their Types

A tactile sensor is a device that can measure quantity or property upon physical contact with any object. Some definitions say that a tactile sensor can only measure force, but it is not limited to force, any quantity which can be detected upon physical contact using a sensor can be referred to as a tactile sensor. The shape of the object, the texture of the object, temperature, moisture and pressure can also be some physical quantities that can be measured using tactile sensors [16]. This study focuses on the design, fabrication and experimental characterization of a tactile force sensor for robotic surgical systems.

1.4 Characteristics of a Tactile Sensor considering Robotic Surgical System

Keeping in view the robotic surgical systems the size of the tactile sensor must be compliant with surgical tools. The sensor must be able to detect and decouple force components in 3D space. It will be better that a sensor should detect angular shear forces with a greater resolution to obtain a better idea of grasping forces or contact forces while its application. The sensor must be sensitive to dynamic forces because in robotic surgeries there can be any type of input force whether it can be static or dynamic. Moreover, low hysteresis and better repeatability are also some concerns when designing tactile sensors for surgical robotic systems and tools. The tactile sensor

which is being used in the robotic surgical system must be of biocompatible material and it will be better if it is disposable.

Figure 1.3 A wearable tactile sensor for object grasping feedback [17]

1.5 Application of Tactile Force Sensors in Robotic Surgical Systems

The tactile force sensors can be used in endoscopic probes and surgical palpation probes which can be used for tumor stiffness detection and cancerous tissue removal as a result a better idea of contact force can be acquired. In laparoscopic surgeries, tactile sensors can be mounted on surgical grippers and forceps for the assessment of the applied force and direction of force when surgery is being performed. During the ocular massage in anesthesia training models, the tactile force sensor can be used to measure the applied force and direction also for needle block device where force applications are required in a gentle way.

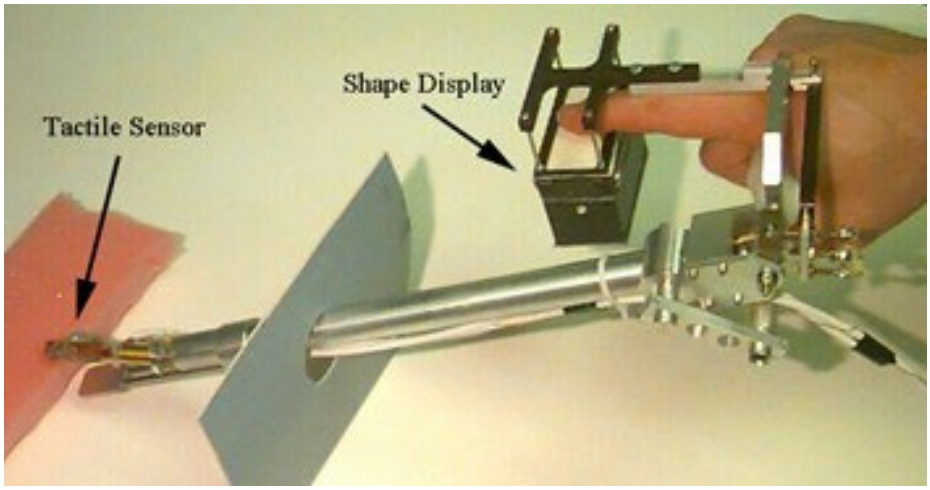

Figure 1.4 A remote palpation probe with integrated tactile force sensor at the jaws of gripper [18]

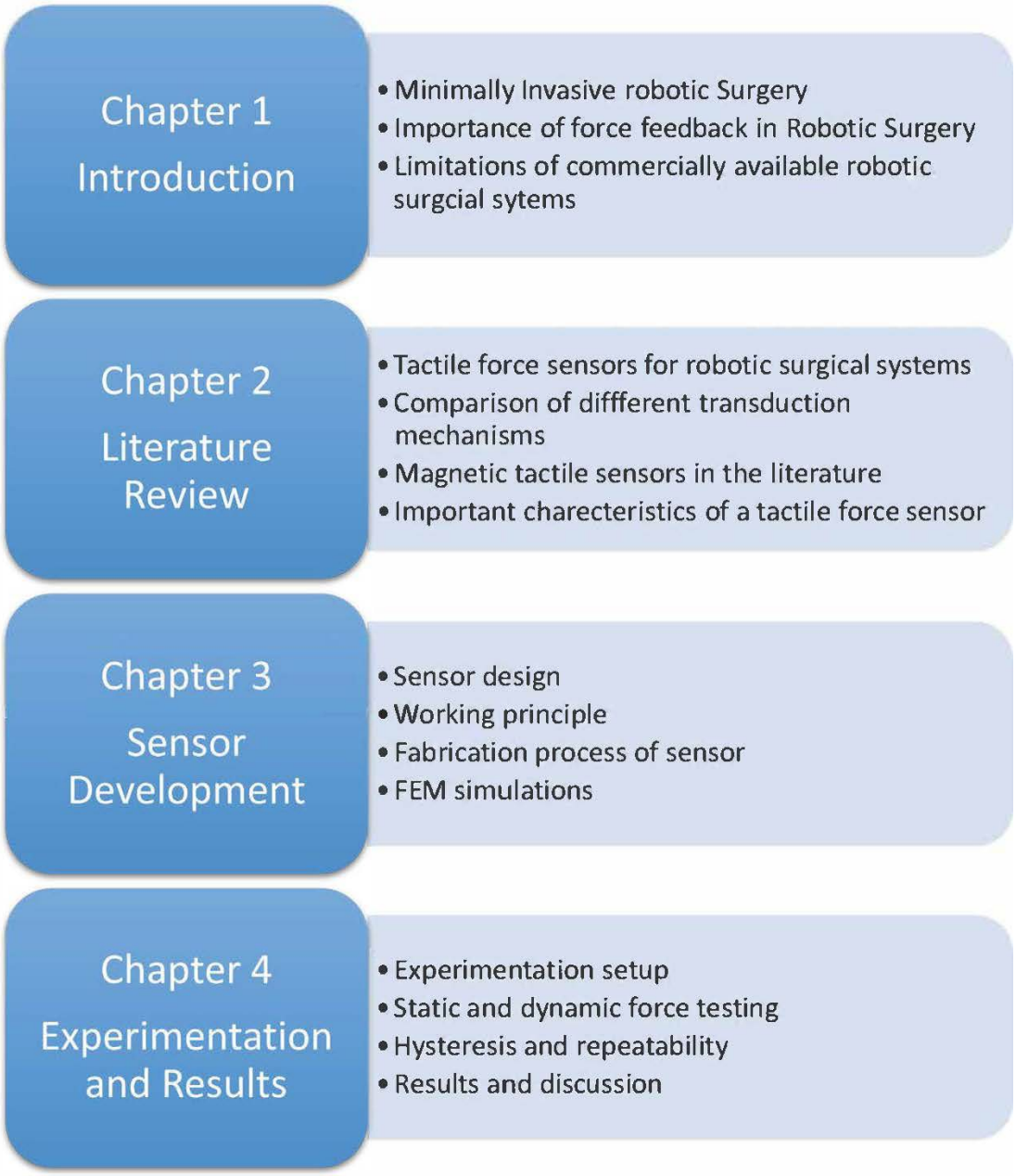

Figure 1.5 Research map of the thesis

Chapter 2: Literature Review

Many different types of tactile sensors exist based on their working principle and transduction mechanisms, for example capacitive, piezoresistive, piezoelectric, inductive, magnetic, and optical. This chapter contains a review of the different tactile force sensors based on the different transduction mechanisms. An extensive literature review of magnetic tactile sensors is included in Section 2.1.6. Moreover, the pros and cons of different transduction mechanisms are also discussed in this chapter.

2.1 Tactile Force Sensors based on Different Transduction Mechanisms

In the literature, tactile force sensors are based on multiple kinds of transduction mechanisms. Based on the design and working principle these tactile sensors can sense forces in single axis and multi axis. The sensing element which is also known as force transfer medium is usually a soft and deformable material so that it can deform to transfer force to the structure used for sensing. In the literature, the sensing element is usually made up of soft materials such as plastics [19], yarns/fabrics [20], and silicone elastomers [21]. These soft materials must be biocompatible keeping in view the robotic surgery so that it should not disturb or damage any body organ. Some of the tactile force sensors based on different transduction mechanisms are discussed below.

2.1.1 Capacitive Tactile Force Sensors

Capacitive sensors use the change in the overlap area of capacitive plates and the change in the gap between the plates to detect the capacitance change depicting shear and normal forces. Zhang et al. 2020 [22] proposed a capacitive tactile sensor (CTS). Stoppers are designed to deter structural deformation when normal forces are applied to realize a high detection sensitivity and wide dynamic range. The sensor provides operation flexibility in normal force detections and unaltered supportiveness on shear force and its angle detections. Different techniques such as higher dielectric materials and needle-like structures are used to increase the sensitivity of capacitive sensors. Liu et al. 2021 [23] presented a flexible 3D tactile sensor using crossbar walls and

micropillar arrays as a dielectric with optimized Young's Modulus. The crossbar structure ensures a fixed overlap area.

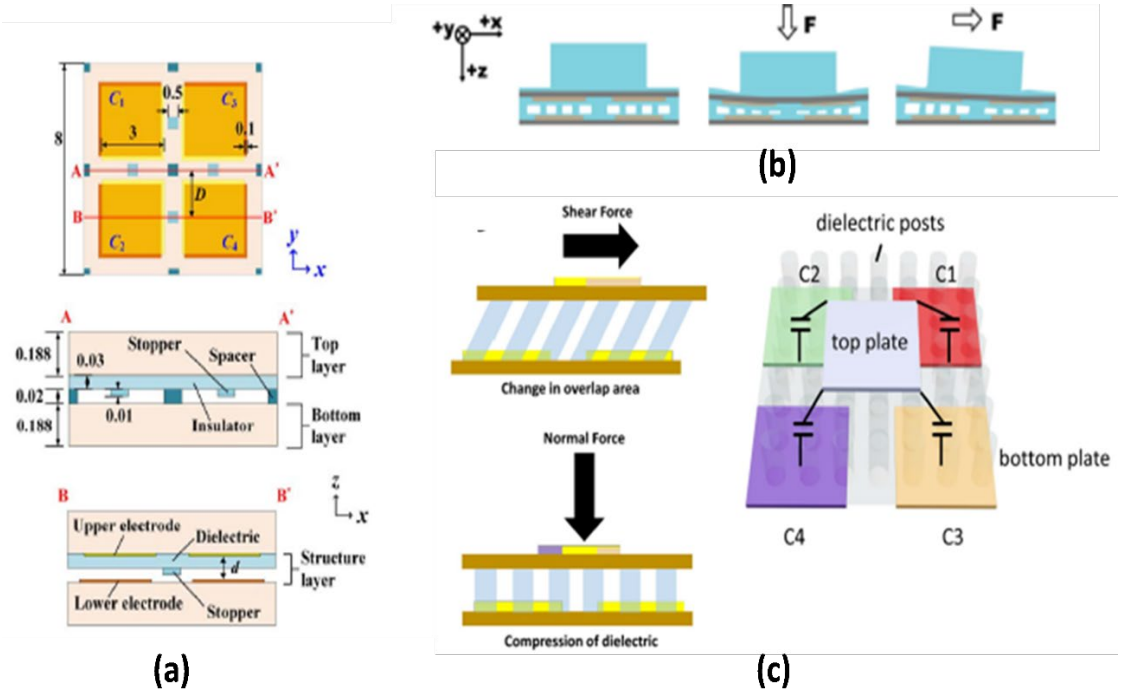

Figure 2.1 (a) Schematics of a capacitive tactile force sensor [21] **(b)** Working principle of capacitive tactile force sensor **(c)** Design of a capacitive tactile force sensor with single top electrode [22]

2.1.2 Piezoelectric Tactile Force Sensors

Piezoelectric sensors use the phenomenon that when stress is applied electric potential is generated across the body. Sokhanvar et al. [24] proposed a MEMS-based piezoelectric sensor for MIS which was utilized for endoscopic instruments. They utilized MEMS-based fabrication technology for PVDF films and MIS graspers mounting. In a similar study for detecting submucosal tumors in endoscopic procedures, Chuang et al. [25] fabricated a tactile sensor based on piezoelectric transduction modality. The sensor was enclosed in soft layers of polydimethylsiloxane (PDMS) and copper ball, PVDF was used as a piezoelectric element. The sensor was incorporated with an endoscopic probe to detect hidden tumors in healthy tissues.

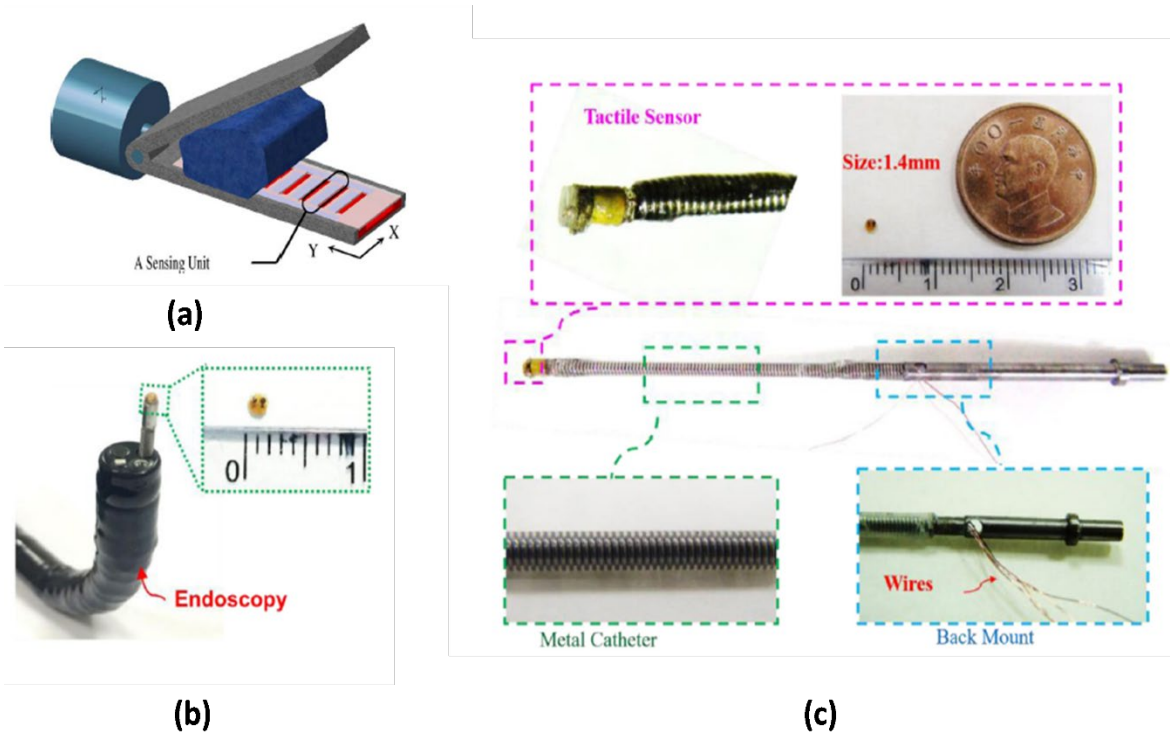

Figure 2.2 (a) PVDF films mounted on a gripper acting as piezoelectric tactile force sensor [23] (b) MEMS based piezoelectric tactile force sensor mounted on endoscopic probe [24] **(c)** Piezo electric tactile force sensor mounted on catheter tip [24]

2.1.3 Piezoresistive Tactile Force Sensor

Piezoresistive sensors use strain gauges [26], [27]. Dargahi and Najarian [13] proposed sensorized graspers with micro strain gauges mounted on the forceps, an electronic feedback system was also developed to analyze the applied force on the LED bar graph. Tanimoto et al. [28] presented a sensor system for intra-vascular neural surgery using micro piezoresistive strain gauges, the sensor was able to measure the interaction force between the catheter and blood vessels. Piezoresistive strain gauges were placed on a silicon diaphragm for sensing, and they tested their sensor on the canine model of an animal. In another effort King et al. [29] Used Flexi Force™ piezoresistive strain gauges on a tool of the da Vinci™ surgical robotic system, they were able to measure grasping forces. Their study explained that the feedback of force in robotic surgery can enhance safety by reducing the gripping forces during the surgical procedures.

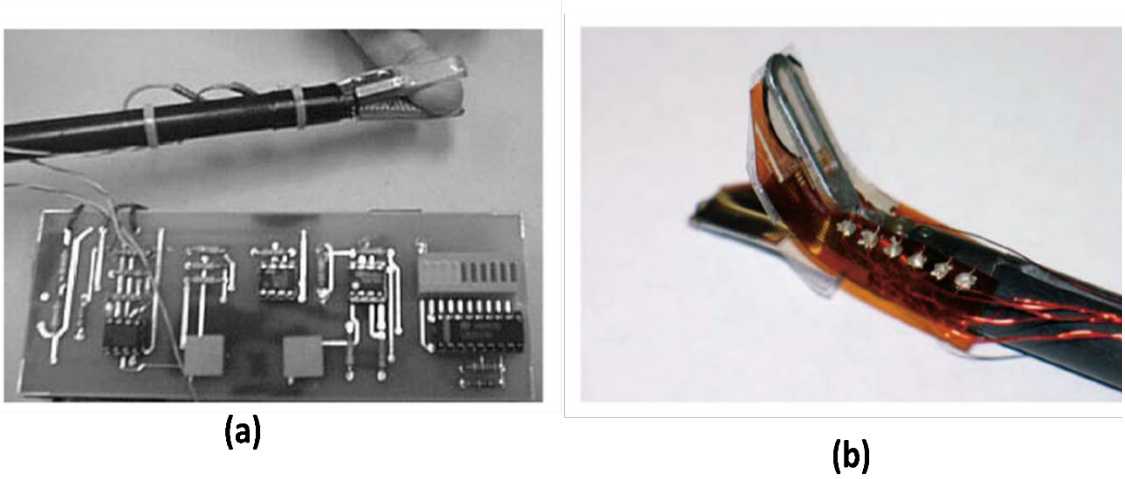

Figure 2.3 (a) Micro strain gauges mounted at grippers with a feedback system for estimating input force [27] **(b)** Flexi force sensors mounted on forceps of daVinci surgical robot [28].

2.1.4 Inductive Tactile Force Sensors

Inductive tactile sensors work on the principle of inductance change due to ferromagnetic marker movement embedded in the elastomer. Kawasetsu et. al. [30] proposed a tactile sensor based on the inductive principle, four round coils were placed on flexible PCB and a soft ferromagnetic marker was embedded in an elastomer. Although no specific application in robotic surgery was not discussed but the sensor was able to measure forces in Normal and shear directions. In another study, Hongbo et. al. [31] presented a similar inductive tactile force sensor but the working principle was a little bit different the inductive coils were the same as proposed by Kawasetsu et. al. [30] but instead of a ferromagnetic marker they used aluminum sheet. The working topology was based on the eddy current effect. The proposed sensor was able to mount on surfaces of grippers because of its small size and flexible PCB layer. It was able to sense both normal and shear forces.

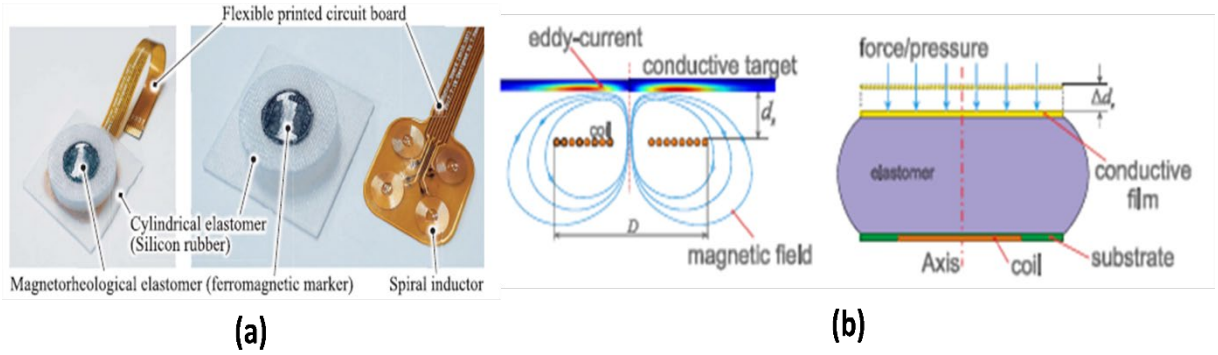

Figure 2.4 (a) A tri-axis inductive tactile force sensor [29] **(b)** Working principle of eddy current

2.1.5 Optical Tactile Force Sensor

Song et. al. [32] presented a novel 3D high-density tactile sensor based on an optical transduction mechanism. The design was inspired by the human eye and can detect normal and shear forces with the sensitivity of 0.000280 mN/Gray and 0.0262 N/µm respectively. The sensor was designed keeping in view the surgical applications and robotic manipulations. Massaro et. al. [33] proposed a MEMS-based optical tactile sensor which worked on the principle of fiber optics. Tasks like roughness detection and shape recognition were also performed by integrating this sensor on a robotic finger.

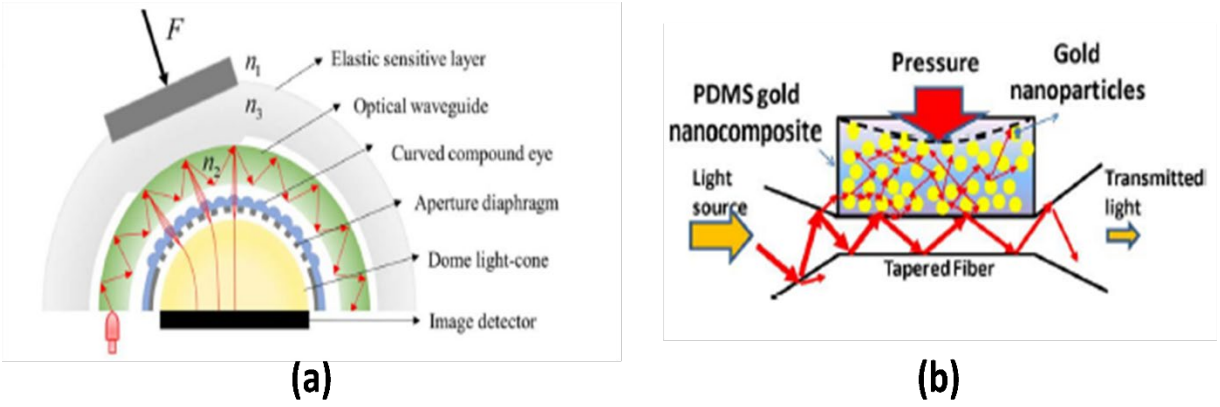

Figure 2.5 (a) Optical tactile force sensor based on bionic eye compound [31] **(b)** A fiber optic-based MEMS force tactile sensor [32]

2.1.6 Magnetic Tactile Force Sensor

Magnetic tactile sensors have gained a lot more importance due to their simple fabrication process, linear output and better output consistency. The first-ever magnetic field based tactile sensors were proposed by Clark et. al. [34] and Nowlin et. al. [35] in the year 1988 and 1991 respectively. Their design comprises Hall sensors and magnets. Later on, many magnetic field based tactile force sensors were presented in the literature with different designs and enhanced sensing capabilities. In 2014 Youssefian et. al. [36] proposed a tactile sensor for achieving force feedback during gripping and grasping robotic applications using Hall sensors. The sensor was able to detect tri-axial forces only at very low force ranges like 1.2 N for normal and 0.2 N for shear forces. The effects of pillar structure and whole bodied elastomers were also discussed using FEM modelling. In another study, Chathuranga et. al. [37] proposed a disposable force sensor for biomedical applications and MIS. The sensor was based on three hall effect sensors placed orthogonally. The magnet was embedded in a soft elastomer so that the sensing range was improved. The displacements were modelled analytically using mathematical formulations. The sensor was able to detect normal and shear forces. Jamone et. al. [38] presented a sensor for the fingers of a robot, they used a single axis hall effect sensor, and the magnet was embedded in the elastomer. The major contribution of this research was improved sensitivity and tactile feedback for robotic fingers. The sensor lacked the multi-axis force sensing capability. The sensor was tested on robotic fingers and the dynamic response of the sensor was also presented but at very low force ranges. Chatzipirpiridis et. al. [39] proposed a magnetic sensor for MIS and it was mounted on a catheter tip to measure tissue stiffness. The proposed sensor was single axis because it was made up of a single hall effect sensor and a single magnet embedded in the elastomer. The catheter was magnetically guided and was tested for a force range up to 0.12 N. A magnetic field principle based tactile sensor which consists of a 3D hall effect sensor was proposed by Wang et. al. [40], the sensor was able to detect tri-axial forces. FEA modelling was used to estimate the position of the magnet in 3D space. Different sizes of magnets were modelled to see the effect on the sensitivity of the sensor. The force range of the sensor was improved as compared to the literature in this study, but it was not enough for MIS and MIRS. Chathuranga et. al. [41] proposed mathematical modelling of magnetic fields for a three-axis force tactile sensor working on the basis of the magnetic field transduction

principle. In this study, the magnetic field was modelled analytically, and displacement was modelled analytically using the bending and compression theory of the cantilever beam. Finally, the sensor was subjected to testing under normal and shear forces and the sensor performed well up to 2 N but only for normal force because the shear force data has a relatively larger error. A tactile skin based on an array of 3D Hall sensors was presented by Tomo et. al. [42]. The sensor was able to measure forces up to 14 N. Temperature effects on sensor output and hysteresis errors were also reported in the study. Tomo et. al. [43], [44] proposed a skin-like tactile sensor for the robot finger and robotic palm to assess the object grasping and contact force of the iCub humanoid robot. The skin was made up of an array of tri-axis magnetometers. Hysteresis errors and errors due to curved and flat surfaces (SNRs) were also reported in these studies. Kumar et. al. [45] proposed a sensor to measure forces applied to an eyeball during the procedure of (ODM) ocular digital massage used as a technique in the ophthalmic anesthesia training model. The proposed sensor was mounted under the eyeball on a mannequin which helps the surgeon to assess the applied force during the procedure of ocular massage. Four linear hall effect sensors were placed axially where an embedded magnet moves in the 3D printed cone below the eyeball. The sensor performed well for normal forces only. Mohammadi et. al. [46] proposed a study in which a tactile sensing array of tri-axis magnetometers was utilized to estimate contact locations while object grasping. An algorithm based on neural networks and machine learning was used to optimize the contact points. The sensor was mounted on robotic fingers for its testing. Jones et. al. [47] presented a tactile sensing device used for hand splinting working on the principle of magnetic transduction mechanism. FEM simulations were used to obtain high sensitivity and measurement ranges. The sensor performed well for both normal and shear forces.

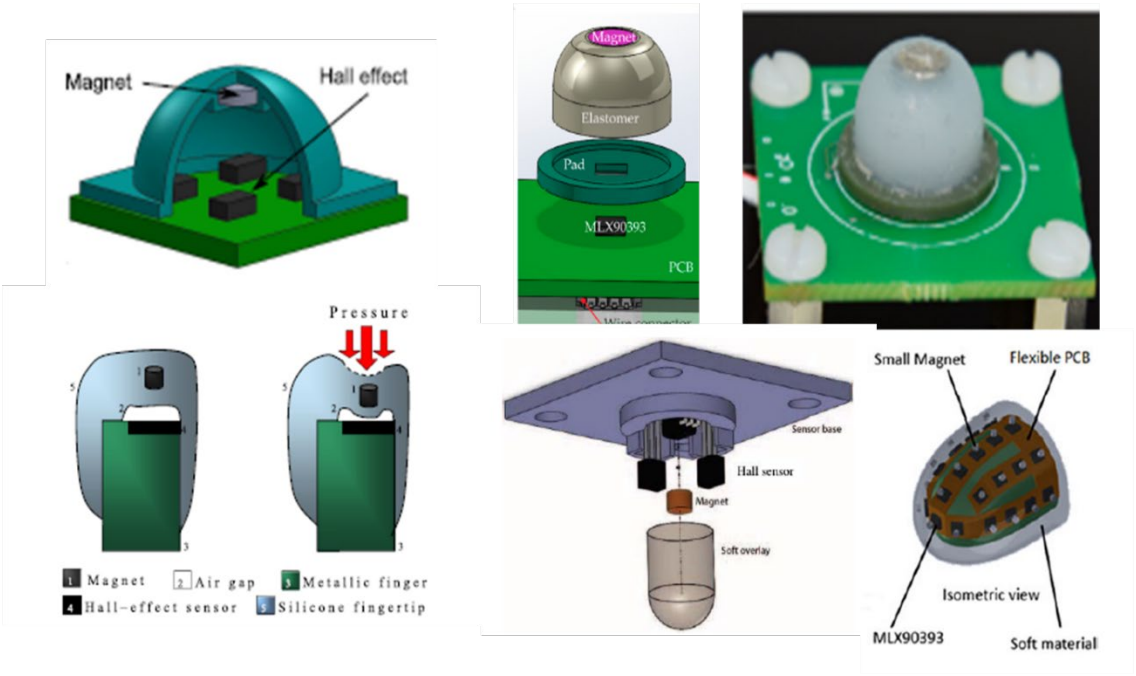

Figure 2.6 Tactile force sensors working on magnetic transduction principle presented in the literature based on single-axis and tri-axis Hall sensors [35][37][39][40][43]

2.2 Comparison of Transduction Mechanisms for Tactile Force Sensing

Table 2.1 contains a comparison summary of tactile sensors based on different transduction mechanisms for robotic surgery, although the tactile force sensors proposed in the literature are small in size, made up of soft materials and able to detect normal and shear forces but the main disadvantages of proposed sensors in literature are hysteresis, nonlinearity, inconsistency in the output readings and expensive fabrication. As compared to other transduction mechanisms, tactile forces sensors which are based on the magnetic transduction principle has many advantages of excellent linearity, better repeatability, low hysteresis, low-cost fabrication, and robustness [1], [48].

Table 2.1 Different transduction mechanisms and their comparison [12,47,48]

Transduction Mechanisms	**Advantages**	**Disadvantages**
Capacitive	Excellent sensitivity, High resolution, High dynamic range, No temperature effects	Stray capacitances, Complex readout electronics, Noise dependency, Large Hysteresis, Non-Linearity
Piezoresistive	Simple fabrication, High spatial resolution, Cost-effective, VLSI compatible	Hysteresis errors, High power consumption, Lack of repeatability, Poor Reliability
Piezoelectric	Excellent frequency response, better accuracy, High sensitivity, Large dynamic range	Poor spatial resolution, Charge leakages, Poor response toward static forces
Optical	Better reliability, large sensing range, High repeatability	Bulky size, Output dependent on temperature or misalignment
Magnetic/Inductive	High linearity, High sensitivity, Large dynamic range, Low fabrication cost	High power consumption, Noise in output signals

2.3 Limitations of the Magnetic Tactile Force Sensors in the Literature

- The magnetic tactile sensors presented in the literature were usually designed for very small force ranges whereas the medical force range for general surgery is 10 N and for laparoscopic surgery, it can go up to 25 N [49].
- In most of the tactile force sensors based on the principle of magnetic transduction mechanisms proposed in the literature the components of force were not decoupled and for MIRS decoupled force feedback can provide enhanced stability while manipulating tasks.
- The designs proposed in the literature were not able to detect shear angular forces which was also a limitation of the magnetic tactile force sensor to detect forces in the 3D space.

2.4 Characteristics of the Proposed Sensor

In this study, an improved tactile force sensor is presented working on the principle of the magnetic field with a goal to achieve a smaller size, cost-effectiveness, large range of force for static forces as well as dynamic forces and a low error of hysteresis. The soft magnetic sensors presented in the literature usually have a hollow cavity in the elastomer causing non-linearity in the output and low force measurement range. Moreover, the proposed sensor can detect and decouple normal, shear and angular forces. The modular design allows changing the soft elastomer layer for achieving different force ranges and sensitivities. The results of FEM simulations are used to optimize the size and placement of the magnets above Hall sensors. The analytical values of magnetic flux obtained through FEM simulations are used to decide the height of the elastomer. These optimized steps helped in achieving highly linear output and a large force measurement range for both static and dynamic applications. The sensor is designed by keeping in mind the requirements of robotic surgery and MIRS.

2.5 Force Requirements for Surgical procedures

As the sensor being proposed in this study is designed with the aim to employ in robotic surgical tools and systems. Therefore, due to variation in different types of surgical procedures the amount of force required for this purpose varies. The detailed

force requirements for different surgical procedures and practices are given in Table 2.2.

Table 2.2 Force requirements in different surgical practices [50]

Type of Surgery	**Average Force (N)**	**Maximum Force (N)**
General Surgery	4.67	11.4
Otorhinolaryngology	8.49	15.6
Obstetrics & gynecology	8.69	10.1
Urology	9.79	15.6

Chapter 3: Sensor Development

The proposed sensor's design, fabrication, and analysis are covered in depth in this chapter. To begin, a design with a new sensing configuration is presented. The materials used in fabrication and the fabrication process are then discussed. The mathematical model of the sensor, as well as the results of relevant FEM based simulations, are then discussed. Each section also expresses aspects of optimization of various design parameters.

3.1 Design and Working Principle of the Sensor

3.1.1 Design

The design of the proposed sensor consists of soft elastomer layers to make the sensor soft and interactable in surgical robotic applications. The two main parts of the proposed sensor consist of a hard base and a soft sensing element. There are four Neodymium N30H magnets having height and diameter of 2 mm and 3 mm respectively which are embedded in the soft elastomer. Four SS39ET Hall sensors which are aligned with the magnets at an offset at the hard FR4 double layer PCB are also used for location estimation of the magnets. The optimized gap through FEM modelling between the Hall sensors and magnets is adjusted by 6 mm. The overall diameter of the proposed sensor is 15 mm. There is a hexagonal dome of a relatively stiff elastomer followed by a hard fiber sheet which enables the uniform force application during the operation of the sensor and hexagonal is used for testing the sensor at different angular forces. The overall height of the sensor with the base PCB, elastomer, magnets and the top hexagonal elastomer is 17 mm. A complete schematic design of the proposed sensor is shown in Figure 3.1.

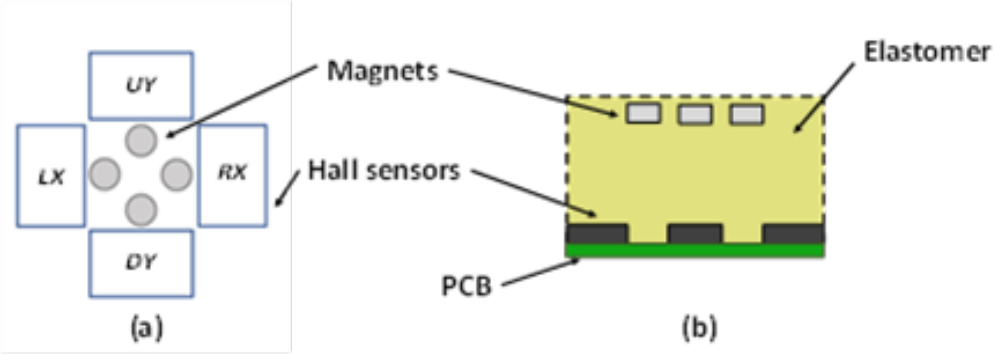

Figure 3.1 Schematics of the proposed sensor **(a)** Top-view **(b)** Cross-section view

3.1.2 Working Principle

In linear Hall effect sensors, a voltage change which is a function of supply voltage can be seen. When a magnetic field is applied across the Hall sensors an increase in voltage can be seen for the north pole of the magnet whereas when the south pole comes near the Hall sensor a voltage decrease can be seen. As shown in Figure 3.1 the proposed sensor consists of four Hall sensors and on top of them, there are four cylindrical magnets at some offset positions. When a normal force is applied on the top face of the sensor all four magnets move in the downward direction. which causes the magnet flux density to increase in all four Hall sensors ultimately a voltage output change is recorded at the output of the *UY*, *DY*, *RX* and *LX* Hall sensors. When a shear force is applied in the +*x*-direction the magnetic field density increases for the RX hall sensor whereas it decreases for the *LX* Hall sensor and remains the same for *UY* and DY Hall sensors. Similarly for positive *y*-direction when the magnets move towards the *UY* Hall sensor the magnetic flux density increases and decreases for the *DY* Hall sensor whereas it remains the same for the *LX* and *RX* Hall sensors. For a force at 45° angle the magnetic flux density at *UY* and *RX* Hall sensor increases whereas it reduces for *LX* Hall sensor and *DY* Hall sensor. The complete sensing scheme at different angles and directions is shown in Table 3.1.

Table 3.1 Magnetic field density towards applied force

Force Direction	Magnetic Field Density			
	B_{RX}	B_{UY}	B_{DY}	B_{LX}
Normal force (z)	↑	↑	↑	↑
Shear force ($+x$)	↑	■	■	↓
Shear force ($-x$)	↓	■	■	↑
Shear force ($+y$)	■	↑	↓	■
Shear force ($-y$)	■	↓	↑	■
Angular force (45°)	↑	↑	↓	↓
Angular force (135°)	↓	↑	↓	↑
Angular force (225°)	↓	↓	↑	↑
Angular force (315°)	↑	↓	↑	↓

3.2 Sensor Schematics and PCB Design

The sensor schematics is designed in proteus 8.6 design suite all the four hall sensors are powered using a common ground and voltage input track the output of all the hall sensors is connected to external connector the schematics design of the sensor is shown in Figure 3.2.

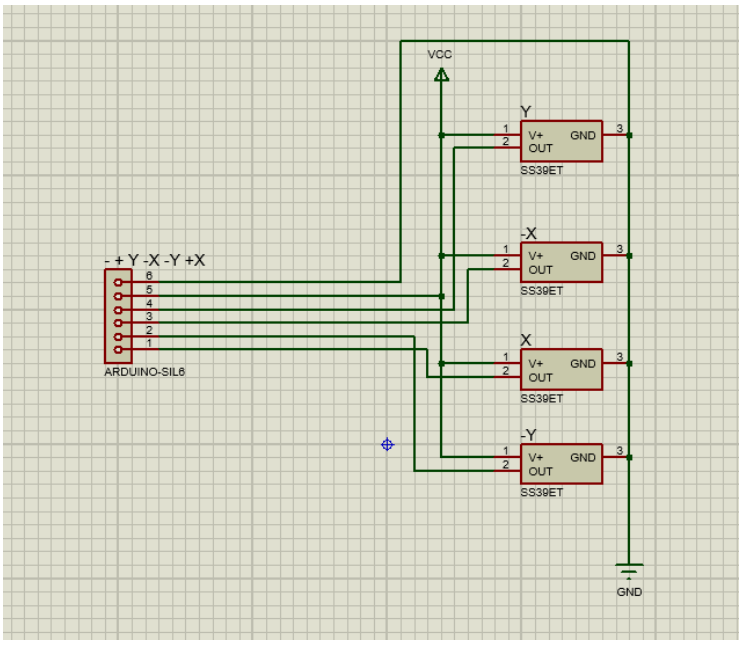

Figure 3.2 Electrical schematic design of the sensor PCB

For the PCB design the track width of T10 is used with a via diameter of 90th and drill diameter of 40th. The routing is done using auto routing feature of proteus. The design rules which were given by the manufacturer were utilized for the accurate fabrication of the PCBs.

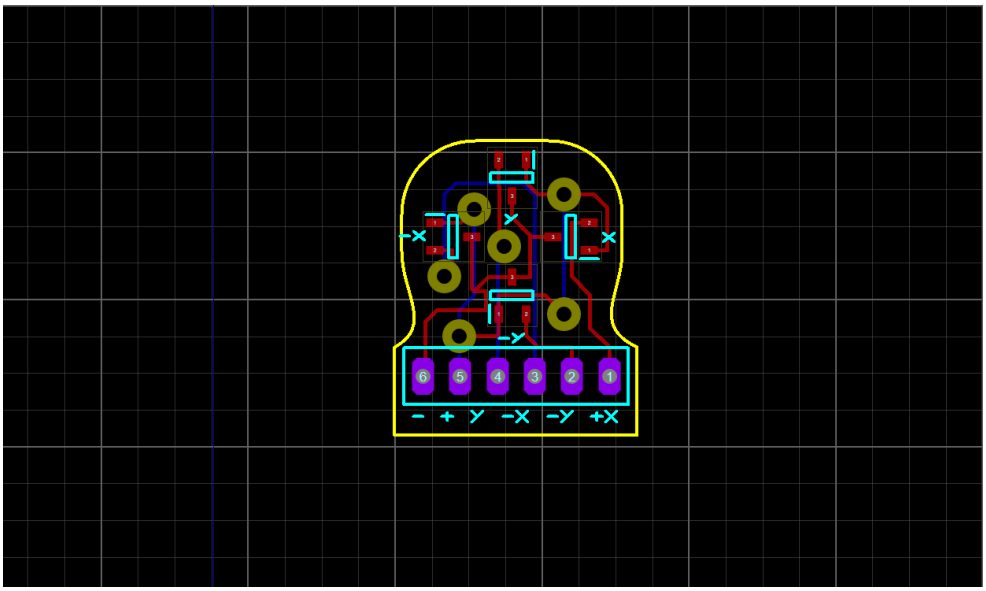

Figure 3.3 PCB design of the proposed sensor

3.3 Sensor Fabrication

Figure 3.4 shows the exploded view of the proposed sensor. The proposed sensor consists of a hard double layer FR4 copper etched PCB which was manufactured by a commercial supplier (PCBWay Inc. China). Four SS39ET Hall sensors are mounted on this PCB using surface mounting technology (SMT) soldering. Two different kinds of elastomer are used for making the soft sensing element of the proposed sensor, one is Ecoflex 00-30 (SmoothOn Inc. USA) and the other is RTV-528 Silicone Rubber. The elastomers are shaped using 3D-printed molds. The Ecoflex 00-30 is liquid silicone rubber that is available in the form of two parts, these two parts are mixed in equal volumetric ratios (1:1) mixed thoroughly and then degassed and poured into the 3D printed molds and then cured for four hours. The RTV-528 rubber is also in liquid form, but it comes with it curing agent. The amount of curing agent is dependent on the curing time, we have used 1% by volume curing agent thoroughly mixed degassed and then allowed to settle in the molds for 24 hours. All the parts of the sensor are assembled with the hard PCB layer using cyanoacrylate glue. The complete fabrication process of the proposed sensor is shown in Figure 3.5.

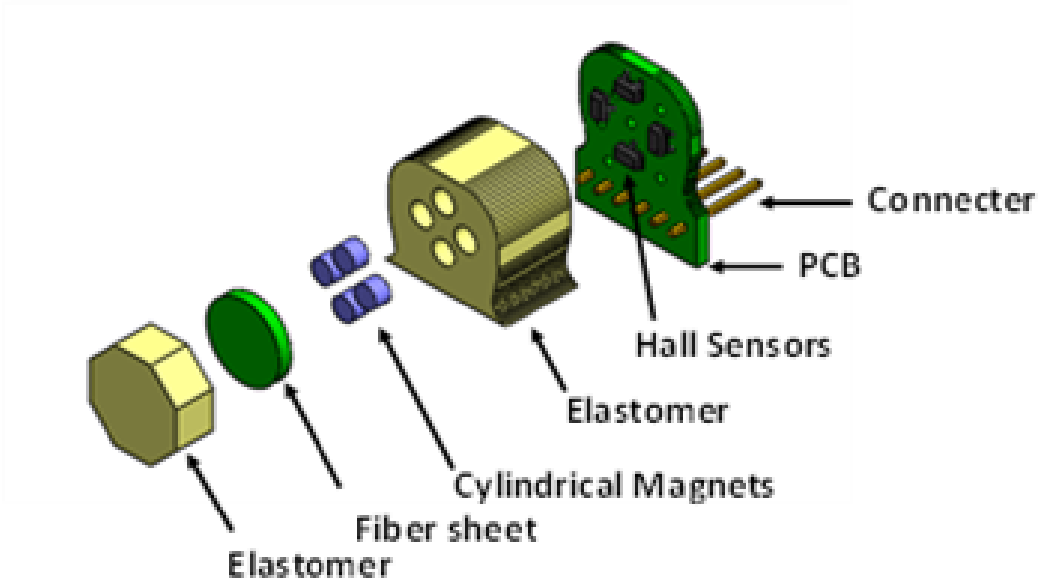

Figure 3.4 Exploded design of the proposed sensor

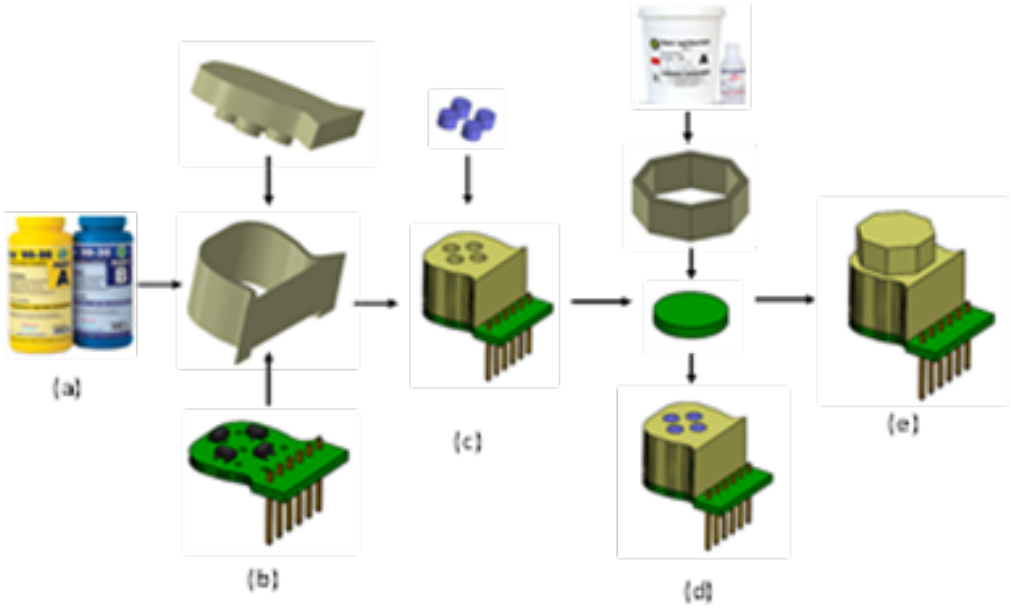

Figure 3.5 (a) Ecoflex 00-30 **(b)** PCB with Hall sensors mounted and 3D printed moulds **(c)** Cylindrical magnets and shaped elastomer on assembled PCB **(d)** Silicone rubber (RTV-528), 3D printed moulds and fibre sheet **(e)** Fabricated sensor.

3.3.1 Cost Analysis

As the sensor is designed and fabricated keeping in view the robotic surgical systems and disposable nature of the sensor required for laparoscopic surgeries [49], the total fabrication cost of the proposed sensor is within $15. Table 3.2 Shows a complete cost

breakdown of the proposed sensor. A complete fabricated sensor is shown in Figure 3.6.

Table 3.2 Cost breakdown for the proposed sensor

Parts	Cost
Two Layered PCB	$2
Hall sensors (SMD)	$6
Moulds (3D printed)	$2
Elastomer	$3
Magnets	$2

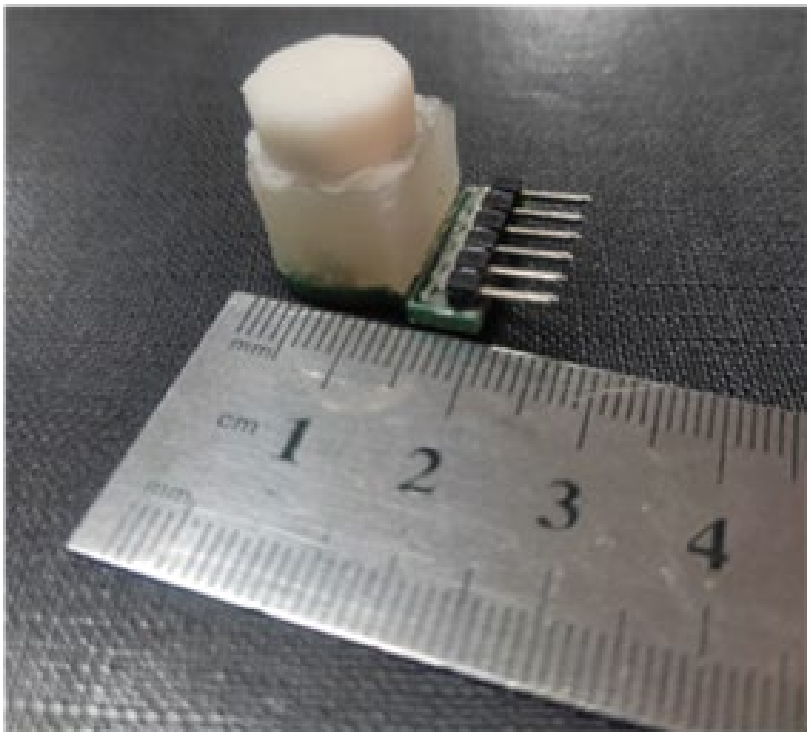

Figure 3.6 Fabricated sensor with a reference object for size estimation

3.4 Sensor Modelling

3.4.1 FEM Modelling

To estimate the effective distance between the Hall sensors and magnets the magnetic field lines from the magnets are plotted using the FEM modelling tool COMSOL Multiphysics. Figure 3.7 shows the lines of the magnetic field from the magnets which

are effectively crossing the hall sensors at a distance of 6 mm. So, the effective distance between the magnets and Hall sensors was adjusted to 6 mm. To achieve a better range and a maximum change in magnetic flux upon the application of force. A confined air space of 20mm × 25mm × 30mm is used to model the magnetic field lines of the proposed sensor.

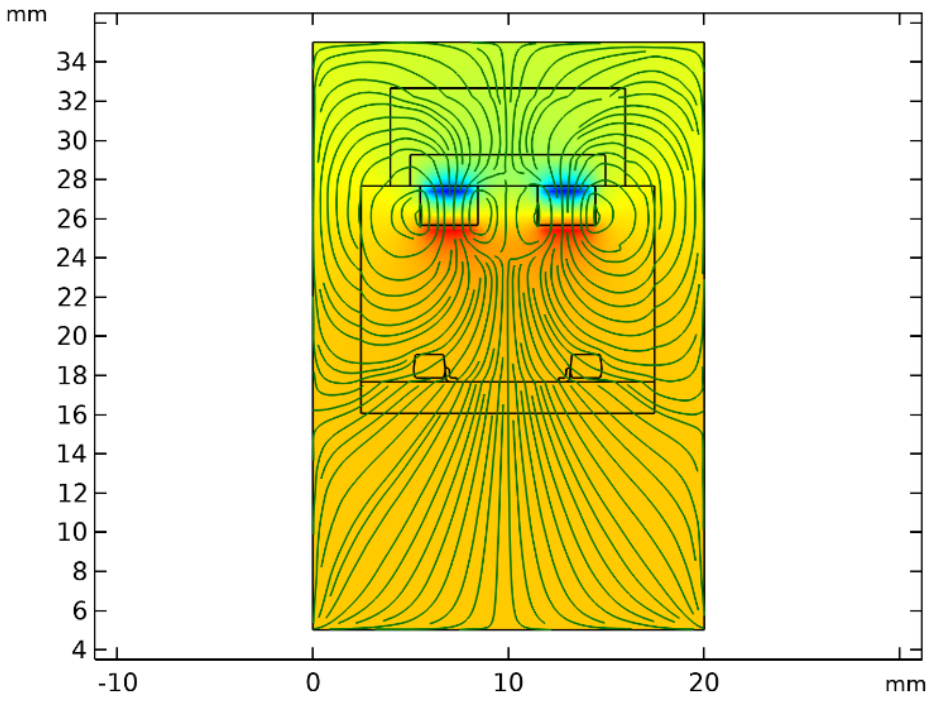

Figure 3.7 Cylindrical magnets embedded in the elastomer emitting magnetic field lines

As already discussed in section 3.1.2 when a force is applied to the proposed sensor the magnetic flux changes across the Hall sensors and to model this phenomenon (solid mechanics) module of COMSOL and (magnetic field no currents) module were used by creating a Multiphysics element. When a normal force is applied on the top face of the sensor the magnetic flux density across all the four Hall sensors shows an increasing trend. Figure 3.8a shows that for a normal force of 20 N the magnetic flux density value shows an increase from 0.00727 Tesla to 0.00764 Tesla.

Similarly, for an input shear force in +*x*-direction, the magnetic response of *RX* and *LX* Hall sensors is demonstrated in Figure 3.8b. The magnetic flux value for the *RX* Hall sensor increases from 0.00727 Tesla to 0.00737 Tesla and decreases with the same ratio for the *LX* Hall sensor.

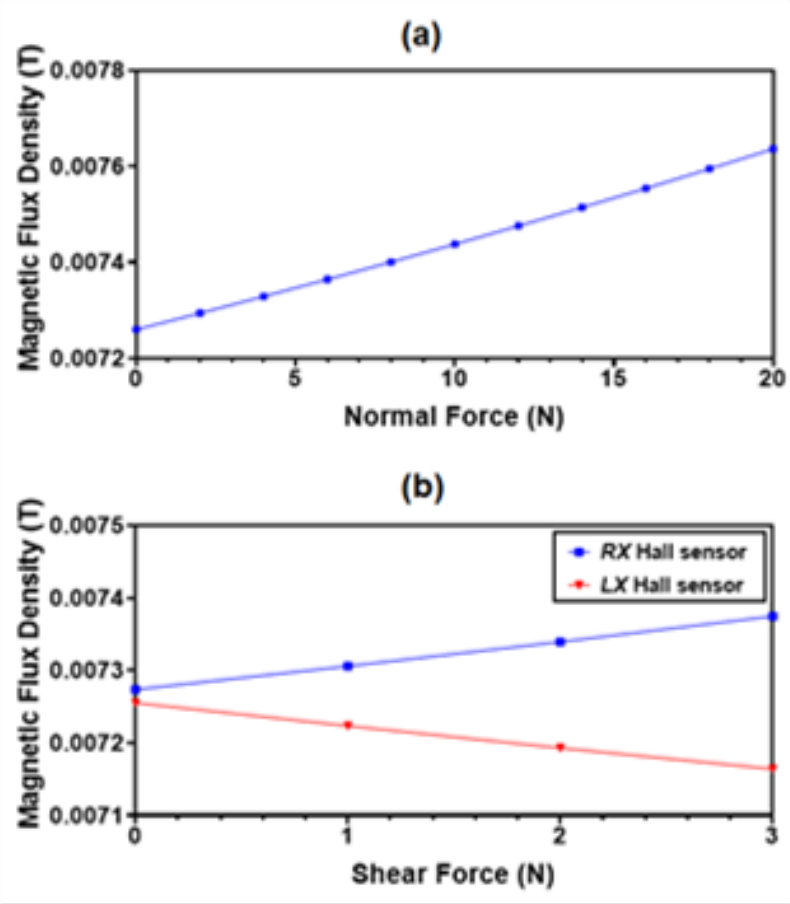

Figure 3.8 (a) Mean magnetic flux across all Hall sensors towards an input normal force **(b)** Magnetic flux across *RX* Hall sensor and *LX* Hall sensor due to a +*x* direction input shear force.

The displacement of embedded magnets in the elastomer is also analyzed using COMSOL solid mechanics modules and the properties of the elastomer used for the analysis are its Youngs Modulus value of 0.1MPa, Poison ratio of 0.49 and density of 1070 kg/m^3 [51]. The analysis shows that the magnets travel a distance of 6 mm distance upon the application of normal force at 20 N and the maximum allowable distance is also 6 mm. So, the maximum force range determined through the FEM analysis is 20 N. Figure 3.8a shows that at a maximum normal force of 20 N the maximum magnetic flux density value is 0.00764. This magnetic flux density value is far less than the maximum sensing capability of the Hall sensors which are being used in the proposed design of the sensor, so this shows that this is not the saturation point of the proposed sensor. To increase the force range the distance between the magnets and Hall sensors can be increased but this will lead to undesired displacements for the shear input forces. Figure 3.9 shows the displacement profile of the proposed sensor.

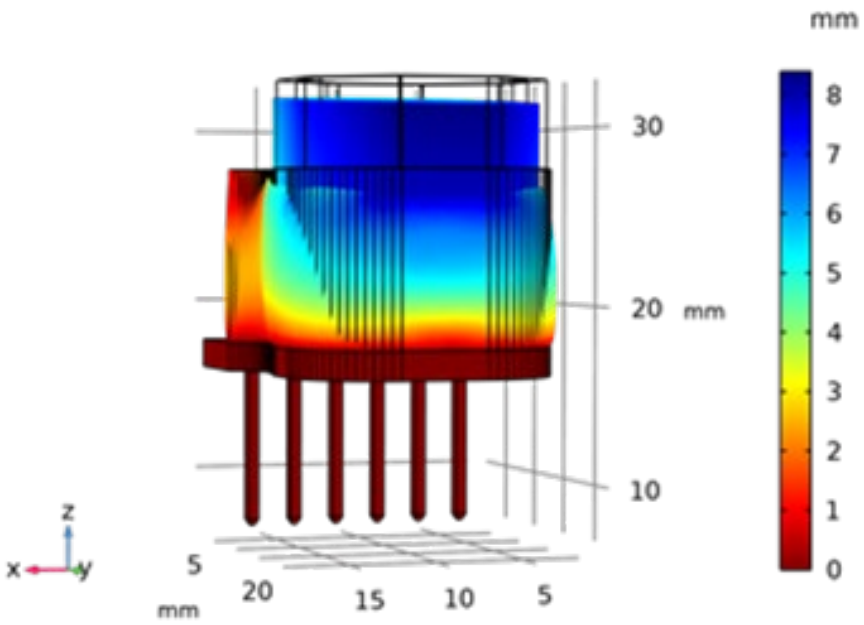

Figure 3.9 Displacement of the proposed sensor simulated using FEM environment

3.4.2 Mathematical Modelling

As discussed in section 3.1.1 the sensor is designed such that it can detect normal, shear and angular input forces and for the decoupling of these force components a set of mathematical equations are modelled for all these forces. Equations (1-3) working principles is based on the differential value of voltage changes and the average voltage change.

$$\Delta V_z = \frac{(\Delta V_{UY}+\Delta V_{DY}+\Delta V_{LX}+\Delta V_{RX})}{4} \quad (1)$$

$$\Delta V_x = \Delta V_{RX} - \Delta V_{LX} \quad (2)$$

$$\Delta V_y = \Delta V_{UY} - \Delta V_{DY} \quad (3)$$

Equation (1) is for the output voltage change for an input normal force. ΔV_z is the output of voltage change whereas an average voltage of all sensors is calculated for this factor. $\Delta V_{UY}, \Delta V_{DY}, \Delta V_{LX}, \Delta V_{RX}$ are the individual Hall sensor voltages from all the Hall sensors. ΔV_x is the output voltage change for an acting input shear force in both positive and negative *x*-directions. Equation (2) works on the principle of differential change in voltage value of the *x*-axis Hall sensors where ΔV_{RX} and ΔV_{LX} are the individual voltage change of the *x*-axis Hall sensors. Similarly, for the input shear force in the *y*-direction Equation (3) works on the principle of differential voltage change of Hall sensors in the y-direction and their individual voltage change ΔV_{UY} and ΔV_{DY}.

$$\Delta V_{45^\circ} = (\Delta V_{UY} + \Delta V_{RX}) - (\Delta V_{DY} + \Delta V_{LX}) \quad (4)$$

$$\Delta V_{135^\circ} = (\Delta V_{UY} + \Delta V_{LX}) - (\Delta V_{DY} + \Delta V_{RX}) \quad (5)$$

$$\Delta V_{225^\circ} = (\Delta V_{DY} + \Delta V_{LX}) - (\Delta V_{UY} + \Delta V_{RX}) \quad (6)$$

$$\Delta V_{315^\circ} = (\Delta V_{DY} + \Delta V_{RX}) - (\Delta V_{UY} + \Delta V_{LX}) \quad (7)$$

For the decoupling of angular input forces Equations (4-7) are used which work on the principle of the sum of the output voltage change of two diagonal Hall sensors with the opposite diagonal Hall sensors. These mathematical equations decouple the forces in the 3D space.

Chapter 4: Experimentation and Results

4.1 Experimental Setup

The proposed magnetic tactile sensor is tested on a tri-axis linear stage of the Denford Fanuc CNC (Computerized Numeric Control) milling machine. A digital force gauge also knows as a push-pull gauge which has a measuring force range of 50 N and has 10 mN resolution is used for precise force application on the sensor which is mounted in the chuck of the machine. The tri-axis stage is manually controlled using the instrument panel of the CNC machine with a minimum displacement resolution of 1µm for static loading. For dynamic loading, the machine is operated in automatic mode using a G-codes based program. The proposed sensor is mounted on the stage of the translation stage. A precise force step size of 10mN is applied during the tests in normal, shear and angular directions. As the output of the proposed sensor is in the form of individual voltage outputs from Hall sensors therefore a National Instruments DAC (Data Acquisition and Control) USB 6009 shown in Figure 4.1 is used as ADC (Analog to Digital Convertor) for recording and analyzing the output response of the sensor. The DAC device is configured with National Instruments LabView Software. A GUI (Graphical User Interface) is also designed to visualize the output response and record the response of the sensor. For filtering and smoothing of the output signals sampling rate of 2 kHz with a maximum of 400 samples are collected and then filtered through 500Hz low pass and smoothing filters. The complete experimental setup for testing and data acquisition is shown in Figure 4.2.

Figure 4.1 USB 6009 DAC device from National Instruments

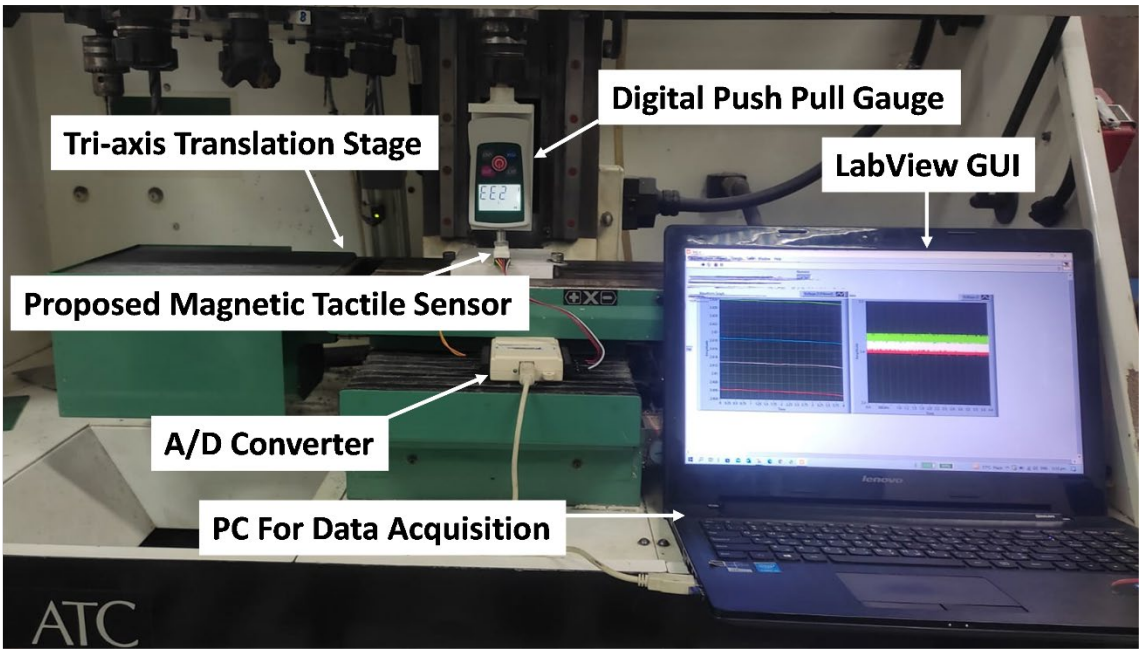

Figure 4.2 Experimental testing and data acquisition setup

4.2 LabView Setup and GUI

For the visualization of the signals without data logging a LabView program is built using the DAQ assistant module. The program consists of two filters signal splitter and displays of waveform graphs and variable indicators. The DAQ Assistant is configured in continuous sampling mode with 48k samples with a sampling frequency of 12 kHz. The maximum voltage range is set between 0-5 V with 4 voltage input channels. A low pass filter is setup with a cut-off frequency of 1 kHz and Butterworth topology of order 3. After this, a half-width triangular moving average filter is used for smoothing. Next to this, a 1 to 4 signal splitter is used for output tracking from all the 4 channels. The GUI consists of a graph of unfiltered and filtered signals and the values of voltages from four different Hall sensors. For the data logging of sensor values for dynamic testing, the excel files are generated with the data and time stamp and were saved using the indexing array and file creation blocks. Figure 4.3 – 4.5 shows the block diagram of the LabView program for real time data acquisition, data logging and GUI for the response assessment of the sensor.

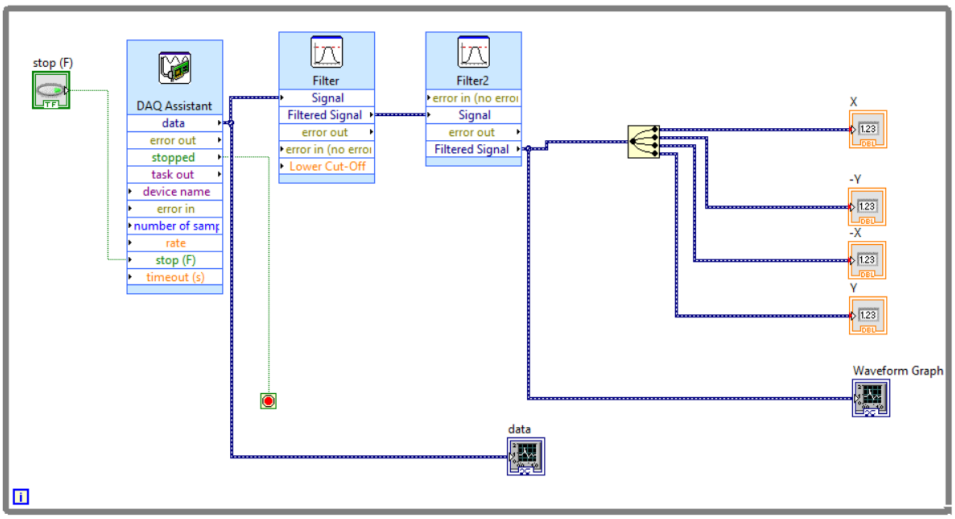

Figure 4.3 LabView block diagram for real time data acquisition of sensor

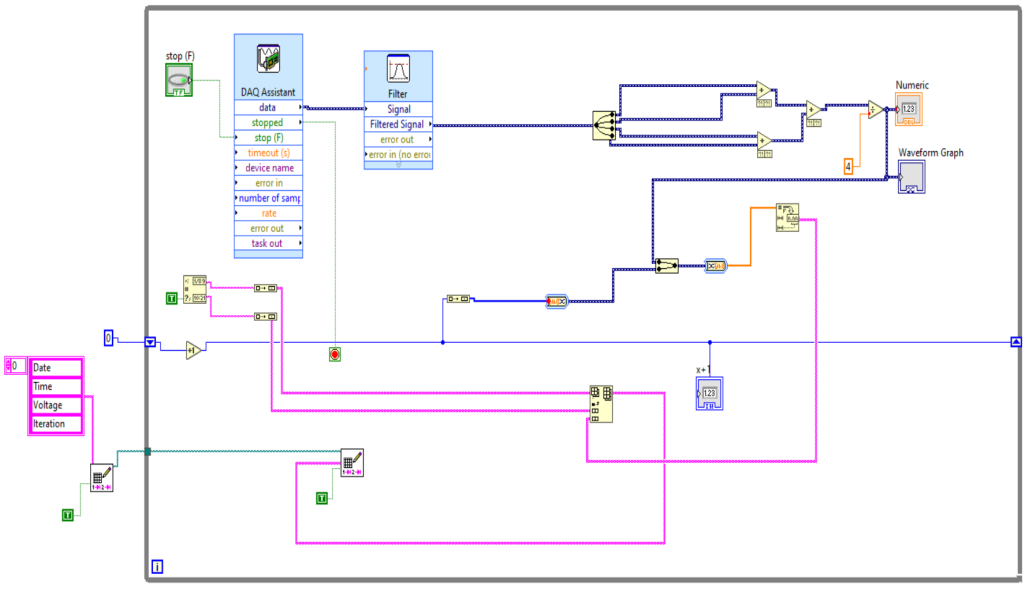

Figure 4.4 LabView block diagram for data logging of the sensor values

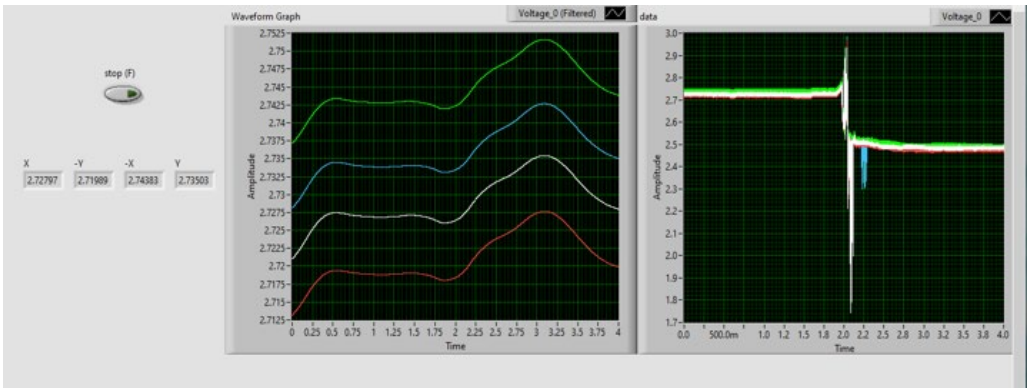

Figure 4.5 LabView GUI for acquisition of the sensor

4.3 Testing and Results

An octagonal-shaped dome on the sensing face of the proposed sensor is designed for the precise application of normal shear and angular forces. Figure 4.6 shows the force direction illustration on the octagonal dome of the proposed sensor. During the force application, the sensor is held stationary whereas the stage moves with the force gauge probe for the application of force. Normal, shear and angular forces with the step size of 0.1N are applied in different tests. After the application of force, a 5s wait time is utilized for readings to get stable. Figure 4.8 shows the recorded displacement response of the proposed magnetic tactile sensor with Ecoflex 00-30 as an elastomer. The displacement response of the sensor is linear for force ranges up to 5N whereas the response beyond this point is nonlinear which is due to the hyper-elastic properties of the soft material Ecoflex 00-30.

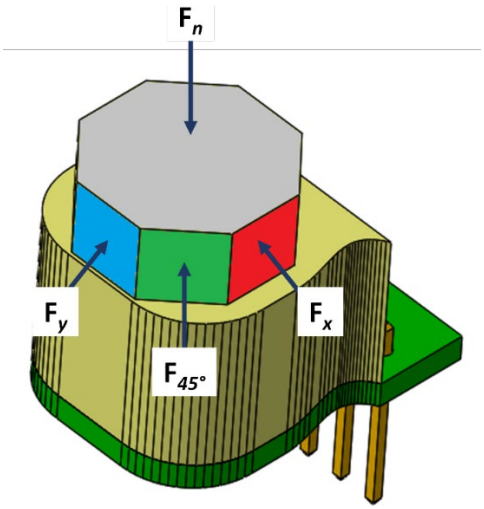

Figure 4.6 Force illustration for octagonal dome

Figure 4.7 Force application on the sensor face using the force gauge probe

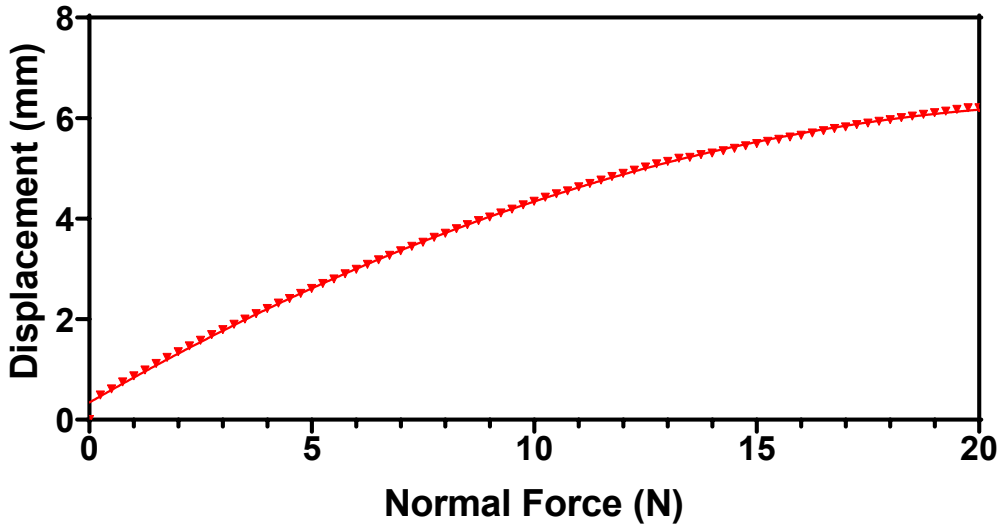

Figure 4.8 Displacement of sensor in normal direction for an input applied force of 20N

4.3.1 Sensor with Ecoflex 00-30 Elastomer

When a normal force is applied on the top face of the proposed sensor shown as a grey color in Figure 4.6 having elastomer as Ecoflex 00-30 all the four magnets embedded in the elastomer move in the normal direction. A voltage change occurs upon the

movement of magnets in the hall sensors. This voltage change is averaged using Equation 1. Figure 4.9 shows the output voltage response of the sensor when a normal force is applied for a force range up to 20 N. At 20 N the maximum allowable distance between the magnets and Hall sensors is achieved which is 6mm. The output response of the sensor is linear perfectly with a maximum output voltage change of 0.325 V at a maximum input force of 20 N. The recorded sensitivity value of the sensor in the normal force direction is 16 mV/N. Figure 4.9 shows that the output voltage response of shear force in the *x*-direction and angular force direction is negligible, this portrays the decoupled response of the proposed sensor.

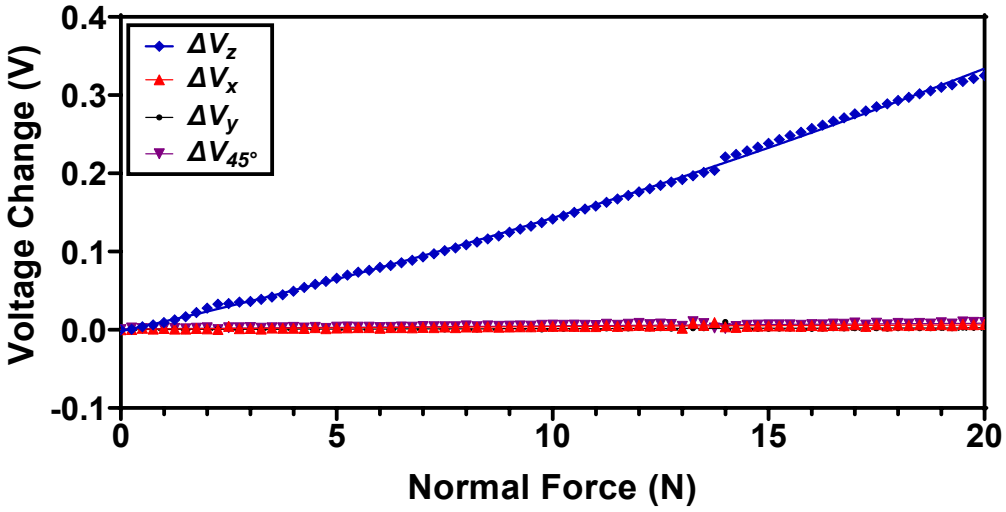

Figure 4.9 Voltage output of the proposed sensor with Ecoflex 00-30 elastomer for a normal force

For a force in the shear direction (+*x*) the sensor is held stationary, and a force is exerted on the red color side face shown in Figure 4.6. The force with a step size of 0.1 N is applied in the shear direction (+*x*). Figure 4.10 shows the response of the sensor for an input shear force range of 3 N. When the force is acting on the sensor on the *x*-axis the output voltage of the *RX* Hall sensor increases and for the *LX* Hall sensor decreases. This individual voltage change is converted to the decoupled response using the mathematical Equation 2. The resultant output voltage response for an input force is the shear direction (+*x*) as shown in Figure 4.10. The recorded sensitivity of the sensor is 30 mV/N for a maximum input shear force range of 3 N. The voltage output response of V_y, V_z and V_{45° remains constant, this behavior depicts the decoupling nature of the proposed sensor.

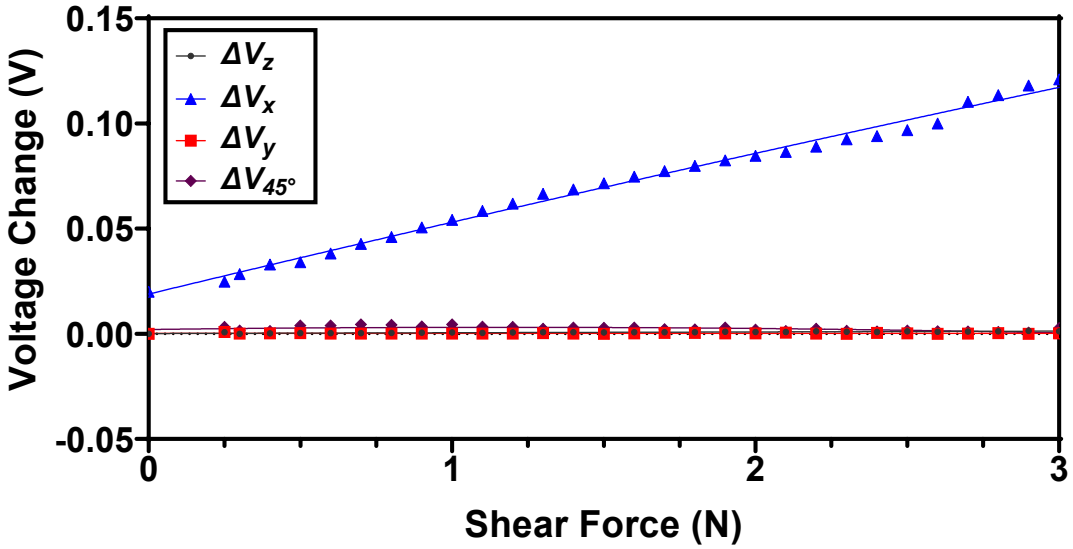

Figure 4.10 Voltage output of the proposed sensor with Ecoflex 00-30 elastomer for a shear force (+*x*)

For the characterization of the sensor for an input force in angular direction (45°) the proposed sensor, the sensor is held stationary, and a force is applied on the green color face shown in Figure 4.6. When the force is applied the magnets move and for the two Hall sensors *RX* and *UY* which are in the direction of magnets movement the voltage output increase whereas it decreases for *DY* and *LX* Hall sensors. Equation 4 is used for calculating the resultant voltage response of the sensor in the angular 45° direction of the force. Figure 4.11 shows the voltage response of the sensor for a 45° angular input force range of 1.5 N. The response of the sensor is perfectly linear with a recorded sensitivity of 81mV/N. The change in voltage using Equations (2) and Equation (3) is minimal because the Hall sensors are positioned in an opposite configuration for the shear axis *x* and *y*. Like the normal force, the applied input force at a 45° angle results in a small change in the output voltage since the output voltage change for the normal force is determined by taking the average voltage response of all the Hall sensors. According to the findings in Figures 4.9–4.11, the proposed sensor design can completely decouple the normal, shear, and acting forces acting on its surface.

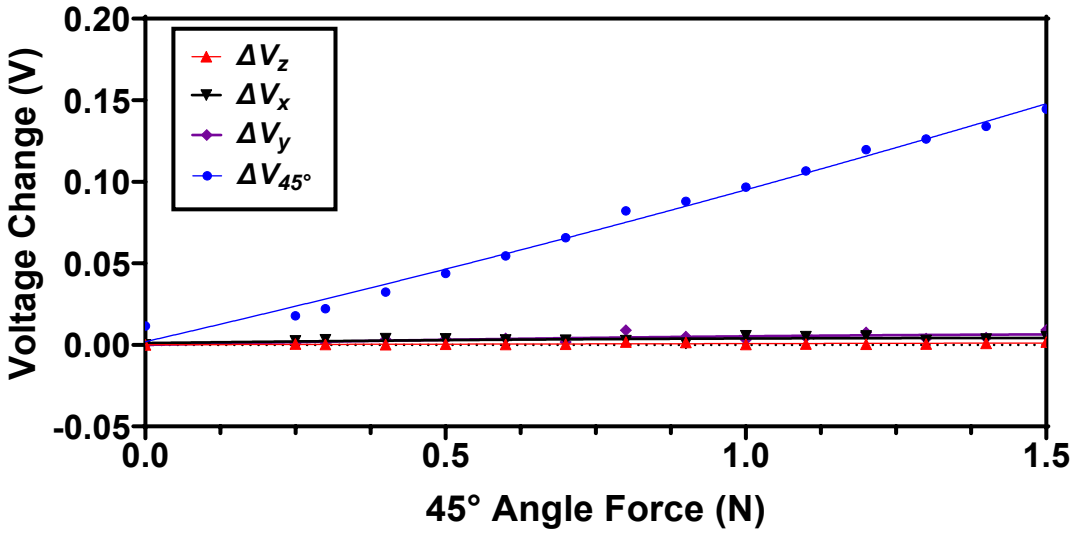

Figure 4.11 Voltage output of the proposed sensor with Ecoflex 00-30 elastomer for an angular force (45°)

The response of the sensor is also assessed by applying different forces at angles of 0°, 45°, 90°, 135°, 180°, 225°, 270°, and 315° to evaluate the behaviour of the proposed sensor in the 3D space. Figure 4.12 shows the measured voltage response of the proposed sensor using the suggested mathematical model in response to various angular forces. Figure 4.12 demonstrates that the presented sensor can detect angular forces in three dimensions. Equation (2) and Equation (3), which operate on the theory of differential change in voltages, show a declining trend for the 180° and 270° angular forces. Maximum variations in voltages are 0.094 V, 0.092 V, 0.0911 V, and 0.0944 V which are acquired for angular forces at 0°, 90°, 180°, and 270° respectively. The voltage response owing to these angular forces is linear perfectly. The voltage changes of 0.169 V, 0.17 V, 0.18 V, and 0.183 V respectively, are recorded for the angular forces at 45°, 135°, 225°, and 315°.

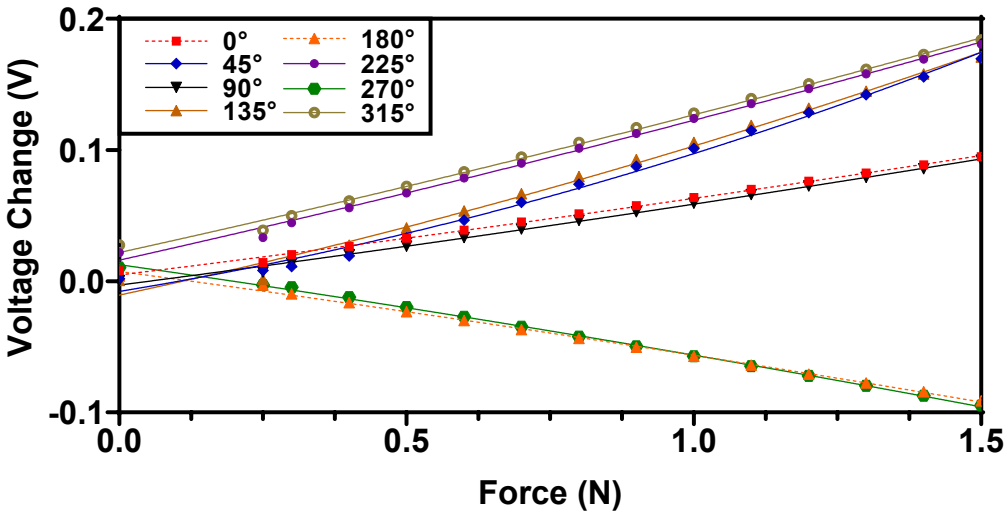

Figure 4.12 Voltage output of the proposed sensor with Ecoflex 00-30 elastomer for input angular forces

4.3.2 Sensor with RTV-528 Elastomer

The proposed sensor having elastomer as RTV-528 is also tested for input forces in normal shear and angular directions. As the force range and sensitivity of the sensor depends upon the stiffness factor of the elastomer, the modular and flexible design of the proposed sensor allows changing the elastomer with respect to the desired force range and sensitivity. The RTV-528 is a stiff elastomer as compared to Ecoflex 00-30, Young's modulus value of RTV-528 silicone rubber is 0.454 MPa and is 0.125 MPa for Ecoflex 00-30. Figure (4.13 - 4.15) shows the response of the sensor for input normal force, shear force (+x) and angular force (45°). As Young's modulus value of RTV-528 is high as compared to Ecoflex 00-30 elastomer therefore a high range of force is achieved that is 50 N in the normal direction, 5.5 N in the shear direction and 4 N in angular is achieved. However, the recorded sensitivity values for normal, shear and angular directions are 2.52 mV/N, 3.4 mV/N and 25 mV/N respectively.

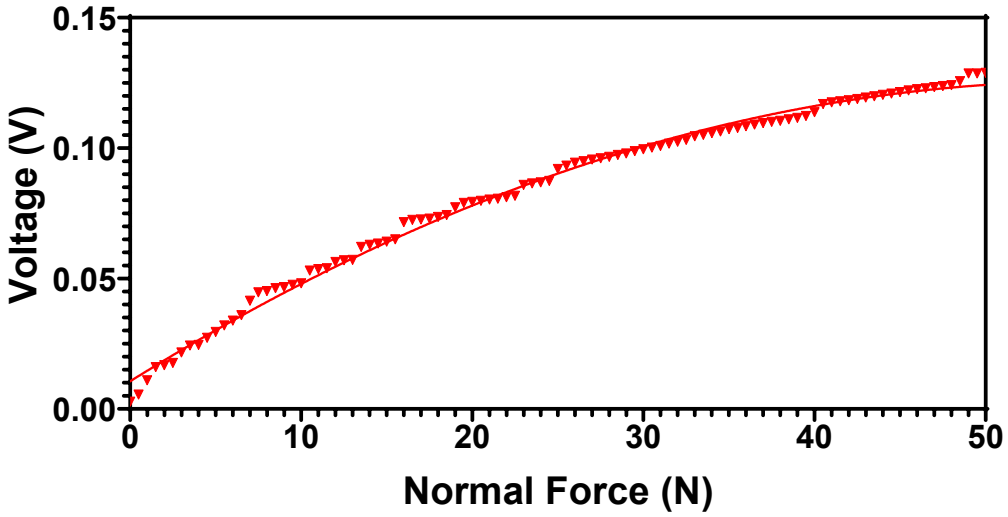

Figure 4.13 Voltage output of the proposed sensor having RTV-528 as elastomer for an input normal force

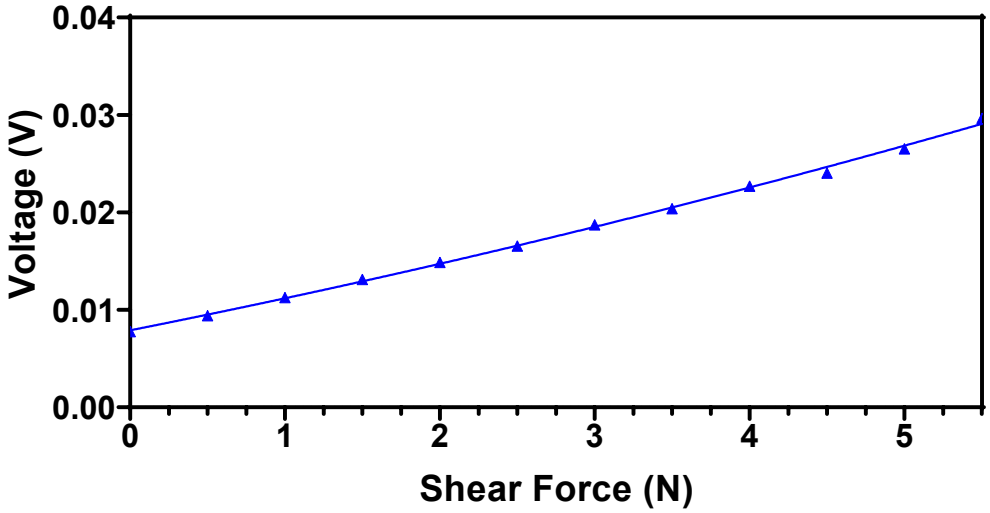

Figure 4.14 Voltage output of the proposed sensor having RTV-528 as elastomer for +*x*-direction input shear force

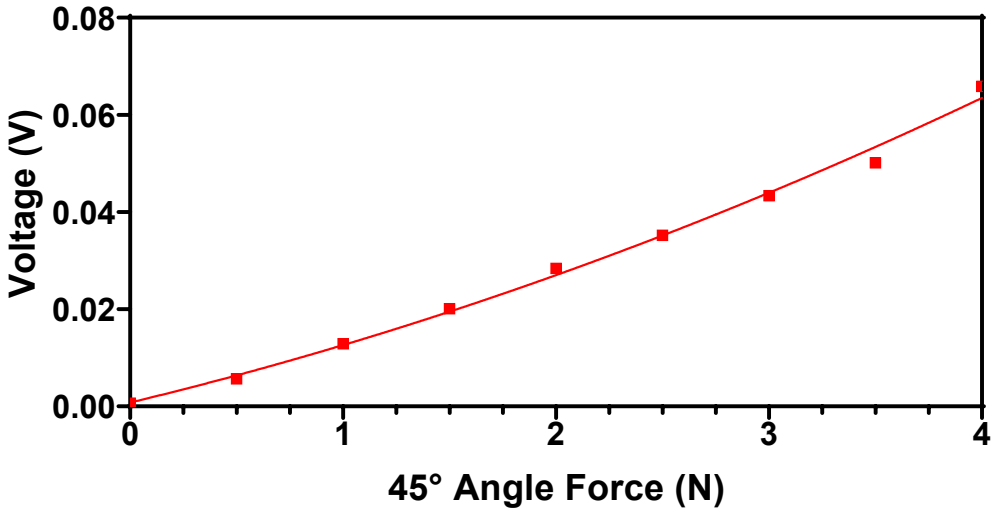

Figure 4.15 Voltage output of the proposed sensor having RTV-528 as elastomer for an input force at 45°

4.3.3 Dynamic Response

The characterization of dynamic forces is an important criterion during robotic surgical procedures; therefore, the sensor must be able to characterize dynamic input forces. The mechanoreceptors in the human hand are of two types and they can measure dynamic contact forces in the ranges of 5Hz to 50Hz and 40Hz to 400Hz. Thus, a tactile sensor that is being employed in a robotic surgical system must be able to detect dynamic forces up to 400Hz [52]. The gripping frequency during the surgical robotic procedure may vary depending upon the type of surgery however, for the laparoscopic surgical procedure gripping frequency of 3Hz is required [53]. The sensor proposed in this study is tested for dynamic forces also. The tri-axis linear stage is translated with a speed of 66mm/s and the probe of the force gauge is impacted on the sensor face for 0.05 s. The total time for a loading and unloading cycle is 0.2 s. The voltage output for a dynamic input normal force of 10 N is shown in Figure 4.16. The results in Figure 4.16 show that a change in voltage of 0.160 V to 0.168 V is recorded for loading and unloading cycles and a dynamic frequency of 4 Hz is calculated for an input normal force.

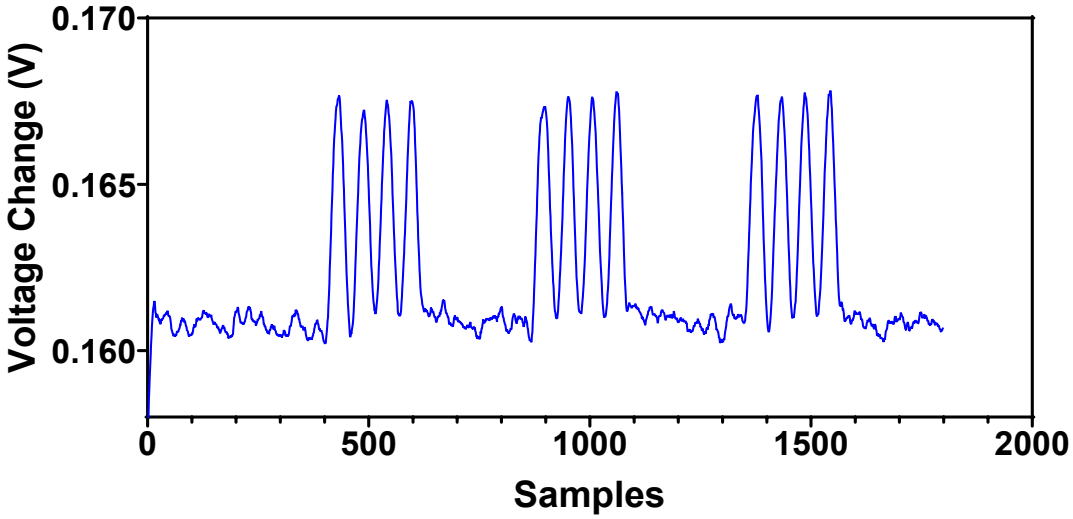

Figure 4.16 Voltage output of the proposed sensor for a dynamic normal force of 10 N

4.3.4 Repeatability Test

The repeatability test of the sensor is an important parameter for the analysis of the output consistency of the sensor which is being employed in robot surgical or biomedical applications [12]. To analyze the repeatability behavior of the proposed sensor it is subject to five consequent loading cycles. Figure 4.17 shows the result of the repeatability test for a normal force range of 20 N. The proposed sensor depicts a very good repeatability characteristic with an error of 6.4%.

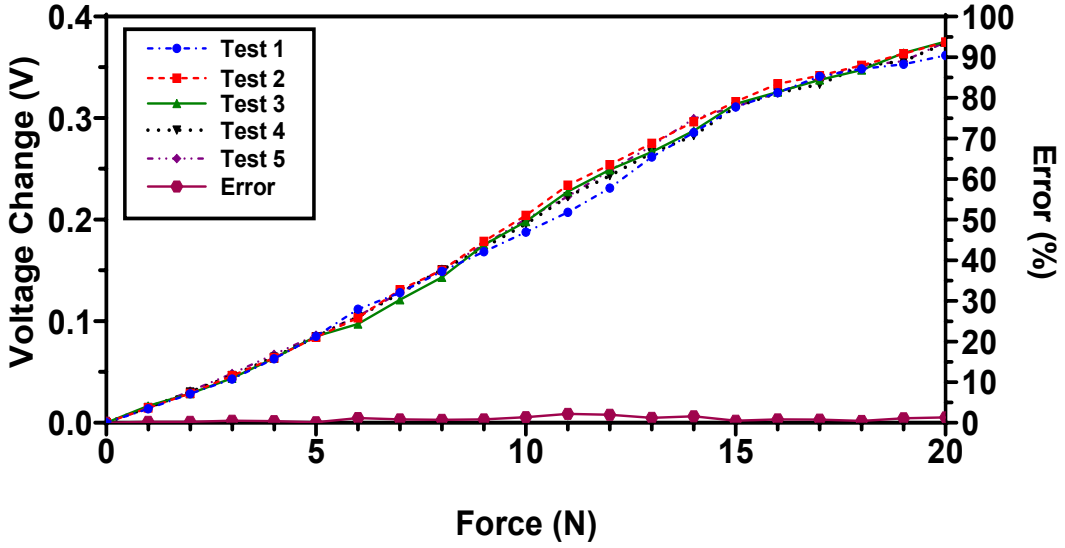

Figure 4.17 Repeatability test of the proposed sensor for a normal force up to 20 N

4.3.5 Hysteresis Test

In the applications in which a fast recovery time of the sensor and dynamic response is required the hysteresis error of the sensor must be very low. The proposed sensor is also tested for hysteresis error for the complete range of input normal force which is 20 N for a loading and unloading cycle. Figure 4.18 shows the response of the proposed sensor for unloading and loading cycles. A hysteresis error of 8.4% is calculated for the complete range of force for loading and unloading cycles. The hysteresis error of the sensor depends on the properties of the soft material or the elastomer and in the proposed sensor Ecoflex 00-30 is a polymer-based elastomer with viscoelastic properties thus it makes the proposed sensor suitable for tactile sensing applications with low hysteresis and fast dynamic response [49].

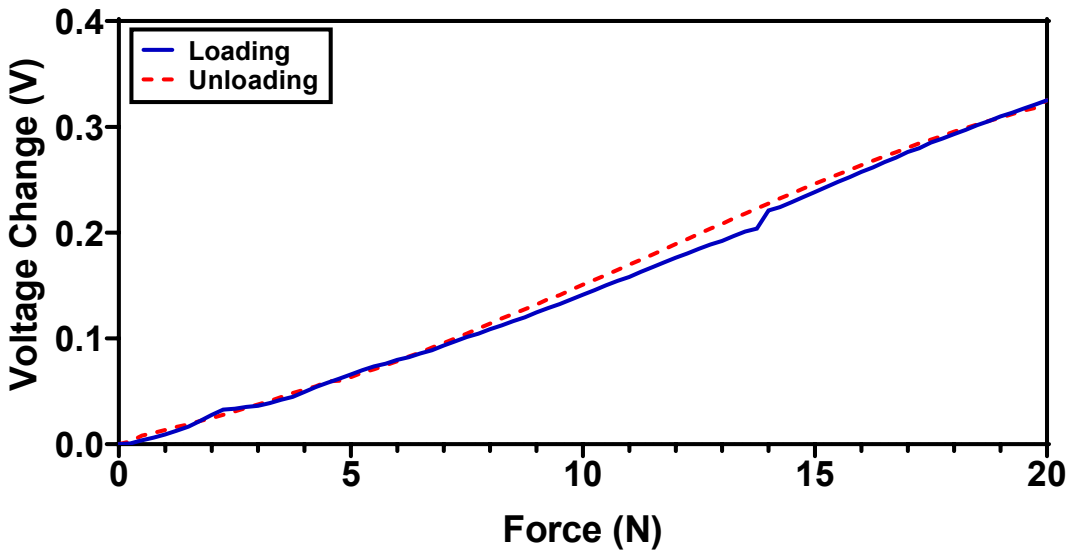

Figure 4.18 Hysteresis of the proposed sensor for a force in normal direction

4.4 Sensor Calibration based on Experimental Voltage Output

As the proposed sensor has an output in the form of voltages and in order to incorporate this sensor with surgical grippers and graspers the sensors output must be in the form of force, so the voltage value of the sensor is required to be converted into force. The sensor proposed in this study is also calibrated for input forces acting on it in all directions. Polynomial type equations are modelled by curve-fitting on the voltage output of the proposed magnetic tactile sensor. The coefficients of the equations are

also derived using the back interpolation model of mathematics. The quadratic formula is used for the conversion of voltage data into force. The derived polynomial equations are given as:

$$\Delta Vz = 0.0003F^2 + 0.0116F + 2.6989 \quad (8)$$

$$\Delta Vx = -0.0073F^2 + 0.0516F + 0.0106 \quad (9)$$

In Equations 8 and 9 ΔV_z and ΔV_x are the output voltage change whereas F is the measured force in normal and shear direction according to the corresponding voltage. To validate the functionality of the proposed mathematical equation the sensor is subjected to input forces of known magnitude and measured forces are calculated using a mathematical model (Equations 8 and 9). Figure 4.19 shows the measured applied force response towards normal force for the proposed sensor using Equation 8. Similarly, Figure 4.20 shows the measured and applied and measured force response for shear force direction using Equation 9. The results show that the applied and measured force for both axes are in close agreement and maximum errors of 4.9% for the normal force and 6.2% for shear force are calculated.

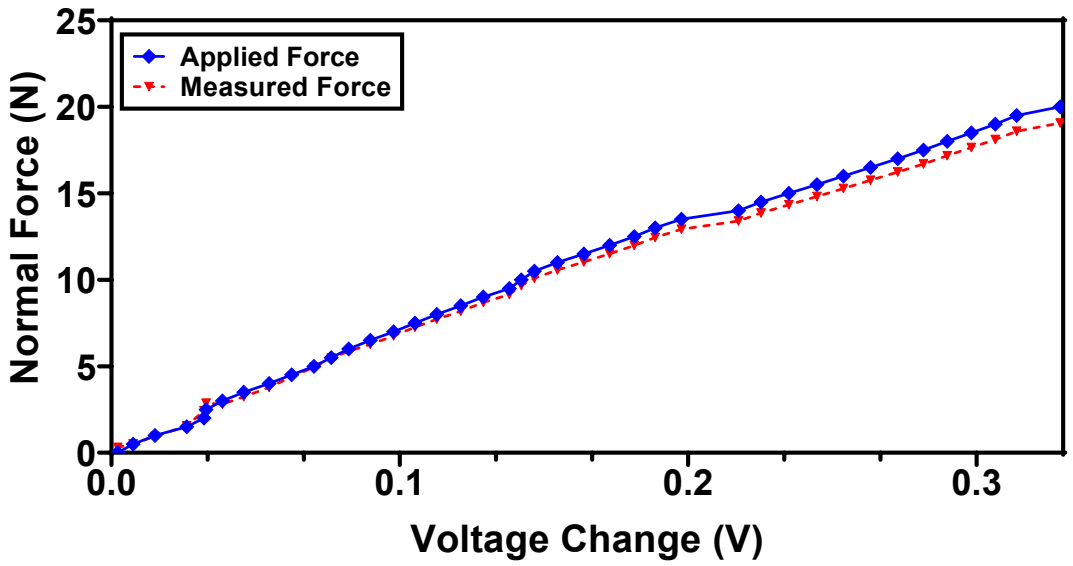

Figure 4.19 Applied versus measured force in the normal direction

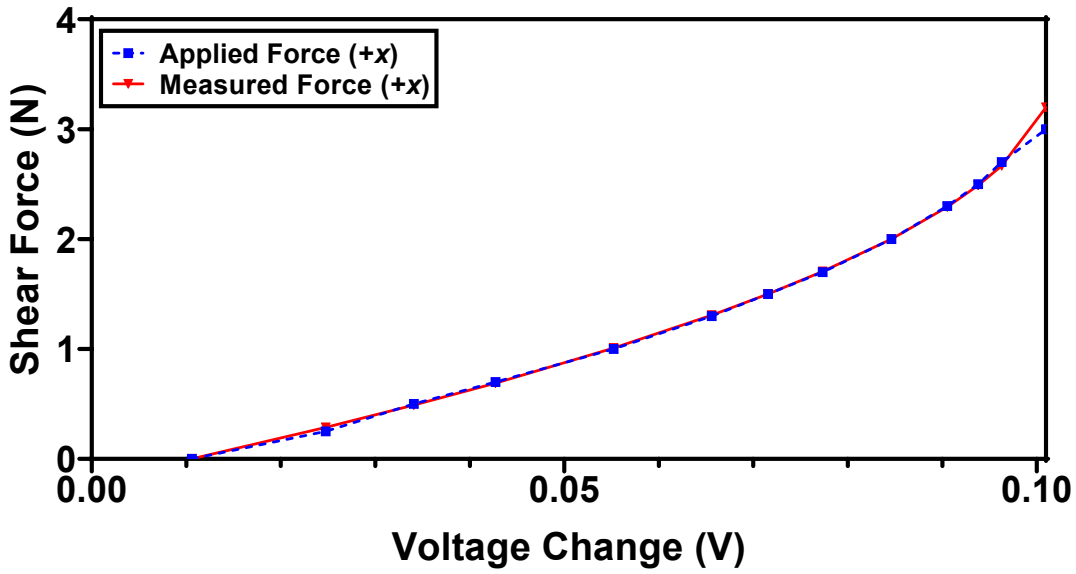

Figure 4.20 Applied versus measured force in the shear direction

4.5 Summary of Performance Characteristics

As the two sensor prototypes are fabricated using two different elastomers, one has relatively less stiffness whereas other has high stiffness. Based on these two different elastomers Ecoflex 00-30 and RTV-528 the performance parameters such as force range, sensitivity and resolution are given in Table 4.1. Both the sensors are able to differentiate between normal force, shear force and angular force and can easily decouple them. The sensor prototype with Ecoflex 00-30 elastomer is also tested for its hysteresis error. The repeatability test for the five cycles is also performed for the characterization of the proposed sensor in terms of output consistency and reliability of the output data. Size of the sensor is in compliant with different kind of surgical grippers and tools such as catheters or probes for palpation.

Table 4.1 Performance parameters of the proposed sensors

Sensor	Elastomer	Force Range	Sensitivity	Resolution
1	Silicone Rubber	Normal (0–50 N) Shear (0–5.5 N) Angular (0–4 N)	Normal (2.52mV/N) Shear (3.4mV/N) Angular (25mV/N)	5mN
2	Ecoflex 00-30	Normal (0–20 N) Shear (0–3 N) Angular (0–1.5 N)	Normal (16mV/N) Shear (30mV/N) Angular (81mV/N)	5mN

4.6 Discussion

Most of the sensors which were proposed in the literature comprise 3D Hall sensors for measuring and decoupling tri-axial forces, but this setup was costly as the 3D Hall sensors are very much more expensive than linear Hall sensors. Moreover, the decoupling of angular input forces was also an issue in the sensors due to the limitation of 3D Hall sensors. The signal filtering, smoothing and data acquisition is also important issue that requires complex protocols in the case of 3D Hall sensors. Table 4.2 provides the comparison of the proposed sensor with the ones proposed in the literature. The comparison shows that the sensor proposed in this study depicts a better force sensing range, good sensitivity and ability to detect and decouple normal force, shear force and angular force. The low hysteresis and good repeatability are some qualities of the proposed sensor that is also an added advantage. The size of the proposed sensor is also comparable with the ones presented in the literature.

As the proposed sensor has advantages of high force measuring range, angular forces measurements, better sensitivity, low hysteresis, and better repeatability as compared to the ones presented in the literature, the modular design of the sensor is also an added advantage. The design of the proposed sensor is robust and therefore no fragile elements such as Hall sensors never come in exposure to the external input force. As the proposed sensor is covered in soft elastomer, therefore during excessive loadings for longer periods cannot damage internal components such as Hall sensors, magnets and PCB. Another major advantage of the proposed sensor design is as there are no electrical connections inside the top-layer of the sensor; hence, the elastomer can deform easily upon any force exertion without causing any damage to wires and fragile

components. The easy to assemble and modular design of the proposed sensor allows changing the elastomer layer upon the desired force range and sensitivities. As discussed in Section 4.2.2 when a high force range of up to 50 N in the normal direction is required RTV-528 silicone elastomer can be used as an elastomer. The proposed design is easy to troubleshoot and also the fabrication cost is very low which is why it can be categorized as a low-cost and disposable sensor.

Table 4.2 Comparison of the proposed sensor with the literature

	Size of Sensor	Elastomer Type	Force Range	Sensitivity	Resolution	Hysteresis
Youssefian et al., [35]	-	Silicone Rubber	(0–1.2 N) Normal force (0–0.2 N) Shear force	-	-	-
Jamone et al., [37]	-	Sylgard 186	(0–3 N) Normal force	0.2 V/N	0.01 N	-
Wang et al., [39]	Diameter: 12 mm Thickness: 12 mm	Ecoflex 00-30	(0–4 N) Normal force (0–1 N) Shear force	-	1.42 mN	3.4%
Chathuranga et al., [40]	Diameter: 15 mm	Dragon Skin 30	(0–2 N) Normal force (0–1.6 N) Shear force	-	-	10%
Tomo et al., [41]	Length: 20 mm Width: 23 mm	Ecoflex 00-30	(0–14 N) Normal force (0–5 N) 45° Shear force	-	-	-
Kumar et al., [44]	Diameter: 30mm	-	(0–30 N) Normal force	1mV/mN	9.8 mN	-
Sensor presented in this work	Diameter: 15 mm Thickness: 17 mm	Ecoflex 00-30	(0–20 N) Normal force (0–3 N) Shear force (0–1.5 N) Angular force	Normal force: 16 mV/N Shear force: 30 mV/N Angular force: 81 mV/N	5 mN	8.4%

4.7 Applications and Future Work

The proposed sensor has many applications, but some important applications include palpation probes for tumor stiffness characterization. The sensor can be mounted on pens and probes for oral cancer screening. Moreover, during the ocular surgical procedures, the proposed sensor can be mounted in ophthalmic anesthesia training models and needle block preparation for an ocular digital massage [45]. The proposed sensor can also be incorporated with surgical grippers and graspers and can be employed in robotic surgical systems and in MIRS for better force estimation and better-grasping stability and control during tissue or any organ manipulation.

Increasing the situational awareness of the surgeon during the robotic surgical procedure is an important issue and one promising way to achieve is to provide haptic feedback on the surgeon console. The future prospect of this study is to develop a haptic feedback device using vibration motors or dielectric elastomer actuators to manipulate the applied force on the sensor to the haptic feedback device. This setup can improve the overall efficiency of the surgical procedures and also will speed up the procedure. The future aim of this study is to propose and develop a surgical pen kind of device that consists of the proposed sensor design with a surgeon feedback console to stimulate the finger of the surgeons during different surgical procedures.

The future work also includes the detection of forces at different angular direction between 0° to 360° by using machine learning and neural networks model training to exactly estimate the input force at any angle. One major addition and contribution to this study in future can be design optimization for achieving high force input ranges in shear and angular directions. The substrate of the proposed sensor is a hard PCB and that can cause in issue while mounting it on even surfaces or round surfaces. Therefore, the substrate or bottom layer of the proposed sensor can be made by using flexible materials such as flexible PCBs and polyimide tapes to make the sensor mounting compliant with rough and uneven surfaces.

4.8 Limitations of the Proposed Sensor

Although the sensor proposed in this study has many parameters and characteristics which make it far better than the ones reported in the literature, but there are some limitations of the proposed sensor. As the proposed sensor works on the principle of

magnetism therefore the environments in which there is an external magnetic field can disturb the output of the proposed sensor. For example, the sensor cannot be used in surgeries involving Magnetic Resonance Imaging or places where external magnetic field is stronger than the magnets which are used in the sensor. Another limitation of the sensor is the hard base or substrate due to this it cannot be mounted on uneven surfaces and that kind of surfaces which require flexible or soft substrate.

Chapter 5: Conclusion

In this study, a meso-scale multi-axis magnetic tactile force sensor for surgical robotic systems is presented. The proposed sensor can measure normal force, shear forces and angular forces. The study focuses on improving the force sensing range referring to robotic surgery by using FEM methods and placements of magnets and Hall sensors. The design of the sensor is modular which allows the elastomers replacement according to the required force range and sensitivities. A force range of 0-20 N in normal direction whereas for shear and angular directions force ranges of 0-3 N and 0-1.5 N respectively are achieved by using the Ecoflex 00-30 as an elastomer. Similarly, when using the RTV-528 as elastomer force ranges of 0-50 N, 0-5.5 N and 0-4.5 N are achieved in normal, shear and angular forces directions respectively. The design of the proposed sensor provides inherent decoupling of normal, shear and angular forces without any crosstalk between the Hall sensors. The maximum error of hysteresis is 8.4% for complete loading cycle and unloading cycle and an error of 6.4% is calculated for the test of repeatability. This makes the sensor suitable for both dynamic and static loading. The proposed mathematical model allows the decoupling of input forces and the back interpolation mathematical interprets the measured force with a very low error. The sensor is manufactured adopting conventional fabrication techniques such as 3D printing thus making it low cost, easy to fabricate and disposable. The sensing face of the sensor is made up of soft and deformable materials because when using it in robotic surgical applications it will not cause any damage to human organs and tissues. The comparable size of the sensor allows its incorporation with surgical palpation probes, surgical pens for tissue stiffness characterization and ophthalmic anesthesia training models.

References

[1] R. S. Dahiya, G. Metta, M. Valle, and G. Sandini, "Tactile sensing-from humans to humanoids," *IEEE Transactions on Robotics*, vol. 26, no. 1, pp. 1–20, Feb. 2010, doi: 10.1109/TRO.2009.2033627.

[2] B. J. Nelson, I. K. Kaliakatsos, and J. J. Abbott, "Microrobots for minimally invasive medicine," *Annual Review of Biomedical Engineering*, vol. 12, pp. 55–85, Aug. 2010, doi: 10.1146/ANNUREV-BIOENG-010510-103409.

[3] S. Uranüs *et al.*, "Early Experience with Telemanipulative Abdominal and Cardiac Surgery with the Zeus^{TM} Robotic System," *European Surgery*, vol. 34, no. 3, pp. 190–193, Jun. 2002, doi: 10.1046/J.1563-2563.2002.T01-1-02049.X.

[4] G. S. Guthart and J. K. Salisbury, "The Intuitive/sup TM/ telesurgery system: overview and application," *Proceedings 2000 ICRA. Millennium Conference. IEEE International Conference on Robotics and Automation. Symposia Proceedings (Cat. No.00CH37065)*, vol. 1, pp. 618–621, doi: 10.1109/ROBOT.2000.844121.

[5] P. Puangmali, K. Althoefer, L. D. Seneviratne, D. Murphy, and P. Dasgupta, "State-of-the-art in force and tactile sensing for minimally invasive surgery," *IEEE Sensors Journal*, vol. 8, no. 4, pp. 371–380, Apr. 2008, doi: 10.1109/JSEN.2008.917481.

[6] R. Ahmadi, M. Packirisamy, J. Dargahi, and R. Cecere, "Discretely loaded beam-type optical fiber tactile sensor for tissue manipulation and palpation in minimally invasive robotic surgery," *IEEE Sensors Journal*, vol. 12, no. 1, pp. 22–32, 2012, doi: 10.1109/JSEN.2011.2113394.

[7] A. M. Okamura, "Haptic Feedback in Robot-Assisted Minimally Invasive Surgery," *Curr Opin Urol*, vol. 19, no. 1, p. 102, Jan. 2009, doi: 10.1097/MOU.0B013E32831A478C.

[8] T. Zhang, H. Liu, L. Jiang, S. Fan, J. Y.-I. sensors Journal, and undefined 2012, "Development of a flexible 3-D tactile sensor system for anthropomorphic artificial hand," *ieeexplore.ieee.org*, Accessed: Feb. 21, 2022. [Online]. Available: https://ieeexplore.ieee.org/abstract/document/6310004/

[9] V. Maheshwari and R. Saraf, “Tactile Devices To Sense Touch on a Par with a Human Finger,” *Angewandte Chemie International Edition*, vol. 47, no. 41, pp. 7808–7826, Sep. 2008, doi: 10.1002/ANIE.200703693.

[10] K. Takei *et al.*, “Nanowire active-matrix circuitry for low-voltage macroscale artificial skin,” *Nature Materials 2010 9:10*, vol. 9, no. 10, pp. 821–826, Sep. 2010, doi: 10.1038/nmat2835.

[11] H. Yousef, M. Boukallel, and K. Althoefer, “Tactile sensing for dexterous in-hand manipulation in robotics—A review,” *Sensors and Actuators A: Physical*, vol. 167, no. 2, pp. 171–187, Jun. 2011, doi: 10.1016/J.SNA.2011.02.038.

[12] M. I. Tiwana, S. J. Redmond, and N. H. Lovell, “A review of tactile sensing technologies with applications in biomedical engineering,” *Sensors and Actuators A: Physical*, vol. 179, pp. 17–31, Jun. 2012, doi: 10.1016/J.SNA.2012.02.051.

[13] S. Najarian, J. Dargahi, and A. Mehrizi, *Artificial tactile sensing in biomedical engineering*. 2009. Accessed: May 08, 2022. [Online]. Available: https://www.accessengineeringlibrary.com/binary/mheaeworks/14b6cc76c087f1ff/80c6d8ec3990c874c07140f32c07c77b57a546e1b236b99b298af07677a257ed/book-summary.pdf

[14] “Robot assisted surgery.jpg - Wikimedia Commons.” https://commons.wikimedia.org/wiki/File:Robot_assisted_surgery.jpg#/media/File:Robot_assisted_surgery.jpg (accessed May 08, 2022).

[15] D. Jones, H. Wang, A. Alazmani, and P. R. Culmer, “A soft multi-axial force sensor to assess tissue properties in RealTime,” *IEEE International Conference on Intelligent Robots and Systems*, vol. 2017-Septe, pp. 5738–5743, 2017, doi: 10.1109/IROS.2017.8206464.

[16] M. H. Lee and H. R. Nicholls, “Review Article Tactile sensing for mechatronics—a state of the art survey,” *Mechatronics*, vol. 9, no. 1, pp. 1–31, 1999.

[17] “World Tactile Sensor Market Report 2025 — Teletype.” https://teletype.in/@swara/t5X0DvUgR (accessed May 08, 2022).

[18] “Remote Palpation Instrument.” http://www.biorobotics.harvard.edu/research/bill.html (accessed May 08, 2022).

[19] S. Khan, S. Tinku, L. Lorenzelli, and R. S. Dahiya, “Flexible tactile sensors using screen-printed P(VDF-TrFE) and MWCNT/PDMS composites,” *IEEE Sensors Journal*, vol. 15, no. 6, pp. 3146–3155, Jun. 2015, doi: 10.1109/JSEN.2014.2368989.

[20] D. Kondo, S. Okada, T. Araki, … E. F.-2011 I., and undefined 2011, “Development of a low-profile sensor using electro-conductive yarns in recognition of slippage,” *ieeexplore.ieee.org*, Accessed: Feb. 21, 2022. [Online]. Available: https://ieeexplore.ieee.org/abstract/document/6094497/

[21] D. Chathuranga, S. H.-2013 I. International, and undefined 2013, “Investigation of a biomimetic fingertip’s ability to discriminate fabrics based on surface textures,” *ieeexplore.ieee.org*, Accessed: Feb. 21, 2022. [Online]. Available: https://ieeexplore.ieee.org/abstract/document/6584336/

[22] Y. Zhang, Y. Jen, C. Mo, … Y. C.-I. S., and undefined 2020, “Realization of multistage detection sensitivity and dynamic range in capacitive tactile sensors,” *ieeexplore.ieee.org*, Accessed: Feb. 21, 2022. [Online]. Available: https://ieeexplore.ieee.org/abstract/document/9088952/

[23] Y. Liu *et al.*, “A flexible capacitive 3D tactile sensor with cross-shaped capacitor plate pair and composite structure dielectric,” *ieeexplore.ieee.org*, Accessed: Feb. 21, 2022. [Online]. Available: https://ieeexplore.ieee.org/abstract/document/9184095/

[24] S. Sokhanvar, M. P.-I. S. Journal, and undefined 2009, “MEMS Endoscopic Tactile Sensor: Toward In-Situ and In-Vivo Tissue Softness Characterization,” *ieeexplore.ieee.org*, Accessed: Feb. 21, 2022. [Online]. Available: https://ieeexplore.ieee.org/abstract/document/5290396/

[25] C. Chuang, T. Li, I. Chou, Y. T.-S. and A. A. Physical, and undefined 2016, “Piezoelectric tactile sensor for submucosal tumor detection in endoscopy,” *Elsevier*, Accessed: Feb. 21, 2022. [Online]. Available: https://www.sciencedirect.com/science/article/pii/S0924424716301650

[26] K. Kim, K. Lee, W. Kim, K. Park, … T. K.-S. and A. A., and undefined 2009, "Polymer-based flexible tactile sensor up to 32× 32 arrays integrated with interconnection terminals," *Elsevier*, Accessed: Feb. 21, 2022. [Online]. Available: https://www.sciencedirect.com/science/article/pii/S092442470900377X

[27] K. Noda, K. Hoshino, K. Matsumoto, and I. Shimoyama, "A shear stress sensor for tactile sensing with the piezoresistive cantilever standing in elastic material," *Sensors and Actuators A: Physical*, vol. 127, no. 2, pp. 295–301, Mar. 2006, doi: 10.1016/J.SNA.2005.09.023.

[28] M. Tanimoto, F. Arai, T. Fukuda, … H. I.-… M. 98. I., and undefined 1998, "Micro force sensor for intravascular neurosurgery and in vivo experiment," *ieeexplore.ieee.org*, Accessed: May 08, 2022. [Online]. Available: https://ieeexplore.ieee.org/abstract/document/659809/?casa_token=1YDNgC3hsEcAAAAA:YcVnWHAusCab3dt1QDfQprH7vRDIIVasS-tXP5eemo6Nd_k0JYWb84cCppscbzr1Y4-zl3MOvUmq

[29] C. King, M. Culjat, … M. F.-I. T., and undefined 2008, "A multielement tactile feedback system for robot-assisted minimally invasive surgery," *ieeexplore.ieee.org*, Accessed: Feb. 21, 2022. [Online]. Available: https://ieeexplore.ieee.org/abstract/document/4674347/

[30] T. Kawasetsu, T. Horii, … H. I.-I. S., and undefined 2018, "Flexible tri-axis tactile sensor using spiral inductor and magnetorheological elastomer," *ieeexplore.ieee.org*, Accessed: Feb. 21, 2022. [Online]. Available: https://ieeexplore.ieee.org/abstract/document/8372916/

[31] H. Wang, D. Jones, G. de Boer, … J. K.-I. S., and undefined 2018, "Design and characterization of tri-axis soft inductive tactile sensors," *ieeexplore.ieee.org*, Accessed: Feb. 21, 2022. [Online]. Available: https://ieeexplore.ieee.org/abstract/document/8374831/

[32] L. Song, H. Zhu, Y. Zheng, … M. Z.-I. T., and undefined 2021, "Bionic compound eye-inspired high spatial and sensitive tactile sensor," *ieeexplore.ieee.org*, Accessed: Feb. 21, 2022. [Online]. Available: https://ieeexplore.ieee.org/abstract/document/9376688/

[33] A. Massaro, F. Spano, … A. L.-E.-I. T., and undefined 2011, "Design and characterization of a nanocomposite pressure sensor implemented in a tactile robotic system," *ieeexplore.ieee.org*, Accessed: Feb. 21, 2022. [Online]. Available: https://ieeexplore.ieee.org/abstract/document/5742700/

[34] J. J. Clark, "Magnetic Field Based Compliance Matching Sensor for High Resolution, High Compliance Tactile Sensing.," pp. 772–777, 1988, doi: 10.1109/robot.1988.12152.

[35] … W. N.-. 1991 I. I. C. on R. and undefined 1991, "Experimental results on Bayesian algorithms for interpreting compliant tactile sensing data," *ieeexplore.ieee.org*, Accessed: May 08, 2022. [Online]. Available: https://ieeexplore.ieee.org/abstract/document/131606/

[36] S. Youssefian, N. Rahbar, and E. Torres-Jara, "Contact behavior of soft spherical tactile sensors," *IEEE Sensors Journal*, vol. 14, no. 5, pp. 1435–1442, 2014, doi: 10.1109/JSEN.2013.2296208.

[37] D. S. Chathuranga, Z. Wang, Y. Noh, T. Nanayakkara, and S. Hirai, "Disposable soft 3 axis force sensor for biomedical applications," *Proceedings of the Annual International Conference of the IEEE Engineering in Medicine and Biology Society, EMBS*, vol. 2015-Novem, pp. 5521–5524, 2015, doi: 10.1109/EMBC.2015.7319642.

[38] L. Jamone, L. Natale, G. Metta, and G. Sandini, "Highly sensitive soft tactile sensors for an anthropomorphic robotic hand," *IEEE Sensors Journal*, vol. 15, no. 8, pp. 4226–4233, 2015, doi: 10.1109/JSEN.2015.2417759.

[39] G. Chatzipirpiridis, P. Erne, O. Ergeneman, S. Pane, and B. J. Nelson, "A magnetic force sensor on a catheter tip for minimally invasive surgery," *Proceedings of the Annual International Conference of the IEEE Engineering in Medicine and Biology Society, EMBS*, vol. 2015-Novem, pp. 7970–7973, 2015, doi: 10.1109/EMBC.2015.7320241.

[40] H. Wang *et al.*, "Design methodology for magnetic field-based soft tri-axis tactile sensors," *Sensors (Switzerland)*, vol. 16, no. 9, 2016, doi: 10.3390/s16091356.

[41] D. S. Chathuranga, Z. Wang, Y. Noh, T. Nanayakkara, and S. Hirai, “Magnetic and Mechanical Modeling of a Soft Three-Axis Force Sensor,” *IEEE Sensors Journal*, vol. 16, no. 13, pp. 5298–5307, 2016, doi: 10.1109/JSEN.2016.2550605.

[42] T. P. Tomo *et al.*, “Design and characterization of a three-axis hall effect-based soft skin sensor,” *Sensors (Switzerland)*, vol. 16, no. 4, 2016, doi: 10.3390/s16040491.

[43] T. P. Tomo *et al.*, “A New Silicone Structure for uSkin - A Soft, Distributed, Digital 3-Axis Skin Sensor and Its Integration on the Humanoid Robot iCub,” *IEEE Robotics and Automation Letters*, vol. 3, no. 3, pp. 2584–2591, 2018, doi: 10.1109/LRA.2018.2812915.

[44] T. P. Tomo *et al.*, “Covering a Robot Fingertip with uSkin: A Soft Electronic Skin with Distributed 3-Axis Force Sensitive Elements for Robot Hands,” *IEEE Robotics and Automation Letters*, vol. 3, no. 1, pp. 124–131, 2018, doi: 10.1109/LRA.2017.2734965.

[45] N. J. Kumar, B. George, and M. Sivaprakasam, “A Sensor System to Assess the Ocular Digital Massage in an Ophthalmic Anaesthesia Training System,” *IEEE Sensors Journal*, vol. 19, no. 22, pp. 10812–10820, 2019, doi: 10.1109/JSEN.2019.2932195.

[46] A. Mohammadi, Y. Xu, Y. Tan, P. Choong, and D. Oetomo, “Magnetic-based soft tactile sensors with deformable continuous force transfer medium for resolving contact locations in robotic grasping and manipulation,” *Sensors (Switzerland)*, vol. 19, no. 22, pp. 1–14, 2019, doi: 10.3390/s19224925.

[47] D. Jones *et al.*, “Design and evaluation of magnetic hall effect tactile sensors for use in sensorized splints,” *Sensors (Switzerland)*, vol. 20, no. 4, pp. 1–13, 2020, doi: 10.3390/s20041123.

[48] C. Chi, X. Sun, N. Xue, T. Li, and C. Liu, “Recent progress in technologies for tactile sensors,” *Sensors (Switzerland)*, vol. 18, no. 4, 2018, doi: 10.3390/s18040948.

[49] W. Othman *et al.*, “Tactile Sensing for Minimally Invasive Surgery: Conventional Methods and Potential Emerging Tactile Technologies,”

Frontiers in Robotics and AI, vol. 8, no. January, pp. 1–43, 2022, doi: 10.3389/frobt.2021.705662.

[50] A. K. Golahmadi, D. Z. Khan, G. P. Mylonas, and H. J. Marcus, "Tool-tissue forces in surgery: A systematic review," *Annals of Medicine and Surgery*, vol. 65, no. March, p. 102268, 2021, doi: 10.1016/j.amsu.2021.102268.

[51] J. Vaicekauskaite, P. Mazurek, S. Vudayagiri, and A. L. Skov, "Mapping the mechanical and electrical properties of commercial silicone elastomer formulations for stretchable transducers," *Journal of Materials Chemistry C*, vol. 8, no. 4, pp. 1273–1279, 2020, doi: 10.1039/c9tc05072h.

[52] Z. Kappassov, J.-A. Corrales, and V. Perdereau, "Tactile sensing in dexterous robot hands — Review," *Robotics and Autonomous Systems*, vol. 74, pp. 195–220, Dec. 2015, Accessed: Jul. 18, 2022. [Online]. Available: https://linkinghub.elsevier.com/retrieve/pii/S0921889015001621

[53] A. Sarmah and U. D. Gulhane, "Surgical robot teleoperated laparoscopic grasper with haptics feedback system," *International Conference on "Emerging Trends in Robotics and Communication Technologies", INTERACT-2010*, pp. 288–291, 2010, doi: 10.1109/INTERACT.2010.5706162.

Completion Certificate

It is certified that the thesis titled "***Development of a Meso-scale Multi-axis Magnetic Tactile Sensor for Robotic Surgery***" submitted by CMS ID. 0000317665, NS Muhammad Rehan of MS-2019, Mechatronics Engineering is complete in all respects as per the requirements of Main Office, NUST (Exam branch).

Supervisor: _____

Dr. Muhammad Mubasher Saleem

Date: ____ August 2022

Thesis Acceptance Certificate

Certified that final copy of MS thesis written by Mr. Muhammad Rehan, (Registration No. 0000317665), of College of Electrical and Mechanical Engineering has been vetted by undersigned, found complete in all respects as per NUST Statues/Regulations, is within the similarity indices limit and is accepted as partial fulfillment for the award of MS/MPhil degree. It is further certified that necessary amendments as pointed out by GEC members of the scholar have also been incorporated in the said thesis.

Signature: _____

Name of Supervisor _____

Date: _____

Signature (HoD): _____

Date: _____

Signature (Dean/Principal): _____

Date: _____